Modern Applications of Solid-state NMR Spectroscopy in Heterogeneous Catalysis

Michael Hunger

Institute of Chemical Technology

University of Stuttgart

School of Materials and Science

Tongji University, Shanghai, P.R. China

April, 2012

Most abundant isotopes with nuclear spin

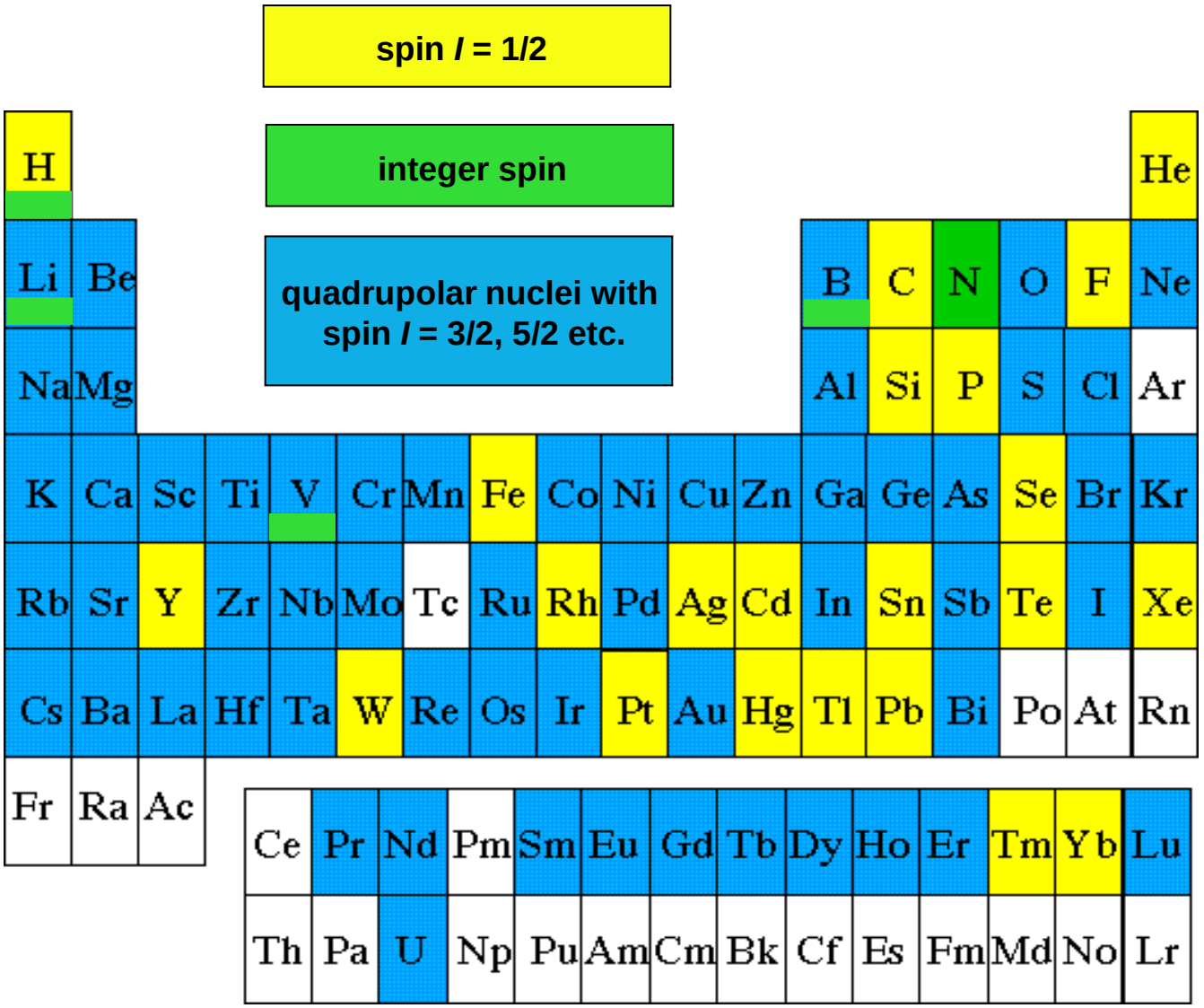

Isotopes interesting for solid-state NMR in heterogeneous catalysis

interesting isotopes (nuclear spin, relative sensitivity in comparison with ^{1}H)

^{1}H (1/2, 1.00), ^{2}H (1, 1.4×10^{-6})

^{13}C (1/2, 1.8×10^{-4}), ^{15}N (1/2, 3.8×10^{-6})

^{31}P (1/2, 6.6×10^{-2})

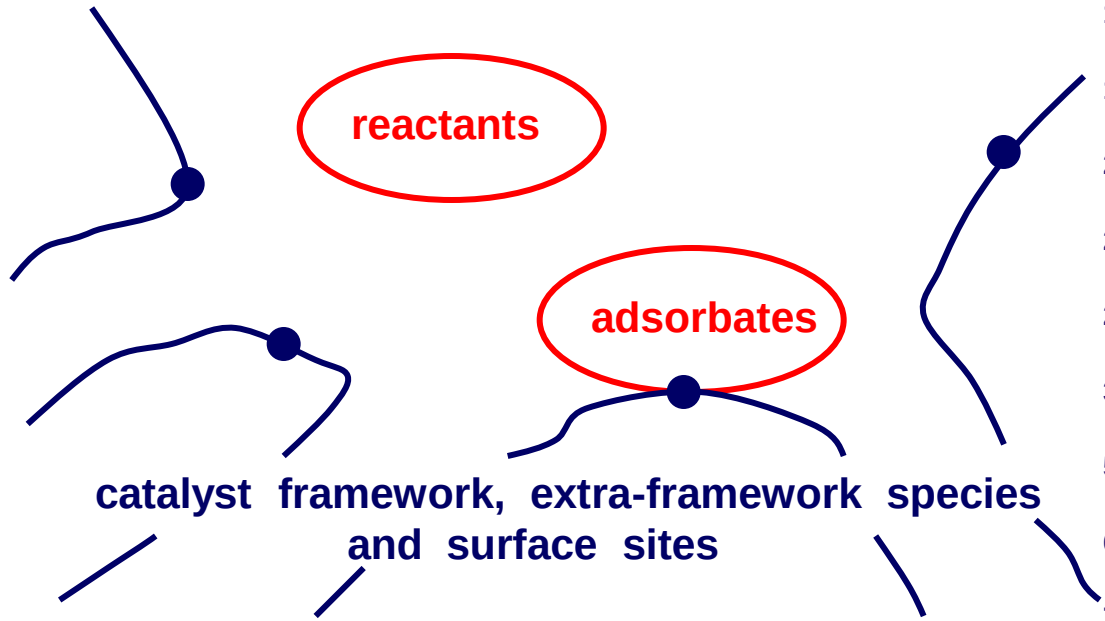

^{7}Li (3/2, 0.27)

^{11}B (3/2, 0.13)

^{17}O (5/2, 1.1×10^{-5})

^{23}Na (3/2, 9.2×10^{-2})

^{27}Al (5/2, 0.21)

^{29}Si (1/2, 3.7×10^{-4})

^{31}P (1/2, 6.6×10^{-2})

^{51}V (7/2, 0.38)

^{67}Zn (5/2, 1.2×10^{-2})

^{71}Ga (3/2, 5.6×10^{-2})

^{133}Cs (7/2, 4.7×10^{-2})

Solid-state NMR of solid catalysts

I. Synthesis of catalysts ⟷
- nature and local structure of framework atoms
- framework defects, amorphous phases and impurities

↓

II. Framework modification ⟷
- incorporation and release of framework atoms
- nature and location of extra-framework species and cations
- anchoring of organic compounds

↓

III. Tailoring of surface sites ⟷
- number, strength, and accessibility of Brønsted acid sites
- presence and strength of base sites
- presence of Lewis acid sites

↓

IV. Catalytic investigations ⟷
- adsorbate complexes and intermediates formed on catalysts
- reaction mechanisms
- reasons of catalyst deactivation

↓

topics I to III

Specific problems of solid-state NMR spectroscopy

Magnetization M_0, Curie's law:

$$M_0 = \frac{N\,\gamma^2\,h^2\,I\,(I+1)\,B_0}{(2\pi)^2\,3\,k_B\,T}$$

detection limit of solid-state NMR is ca. N = 10 µmol spins per gram for ^{1}H nuclei at room temperature

magnetization M_0 decreases with increasing temperature T

broadening of NMR signals due to internal solid-state interactions

most important solid-state interactions:

H_{CSA} : anisotropic shielding of the magnetic field due to the anisotropic electron density in the local structure of the resonating nuclei; $\mathcal{F}$ {LP$^{(2)}$} $\Delta\nu_{CSA}$ up to 50 kHz

H_{DI} : dipolar interaction with magnetic dipole moments of neighboring spins in the local structure; $\mathcal{F}$ {LP$^{(2)}$} $\Delta\nu_{DI}$ up to 100 kHz

H_Q : quadrupolar interaction of the electric quadrupole moment of nuclei with spin I = 3/2, 5/2 etc. with electric field gradients; $\mathcal{F}$ {LP$^{(2)}$ + LP$^{(4)}$} $\Delta\nu_Q$ up to 20 MHz

Techniques of solid-state NMR spectroscopy

spin *I* = 1/2 :

magic angle spinning (MAS)

$\nu_{CSA,\ DI,\ 1QI} = \mathcal{F}\ \{(3\cos^2\Theta - 1)/2\}$

$\rightarrow\ \Theta = 54.7^o$

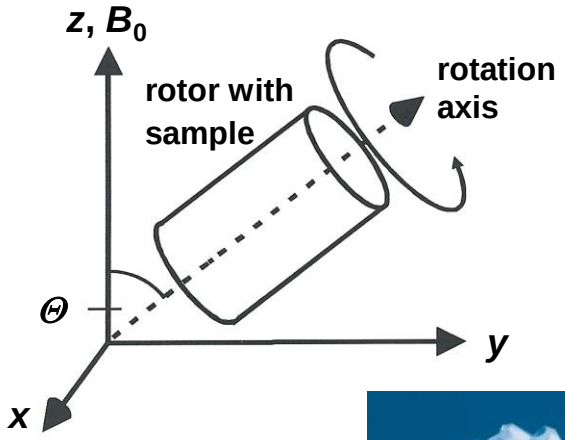

spin *I* = 3/2, 5/2 etc. :

double oriented rotation (DOR)

$\nu_{2QI} = \mathcal{F}\ \{(35\cos^4\Theta - 30\cos^2\Theta + 3)/8\}$

$\rightarrow\ \Theta = 30.6^o$

$\Theta = 70.1^o$

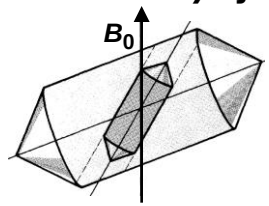

multiple-quantum MAS NMR (MQMAS)

- excitation of three- and five-quantum transitions
- recording of a spin-echo free of anisotropic contributions

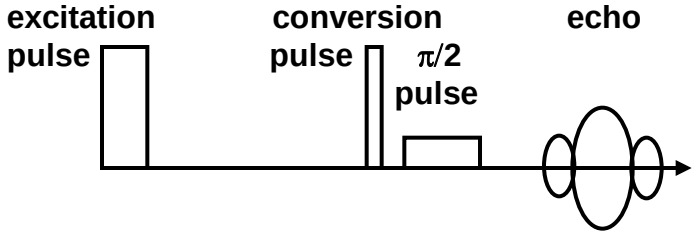

J. Amoureux et al., J. Magn. Reson A 123 (1996) 116

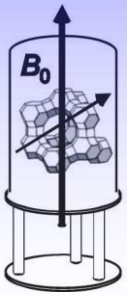

I. Synthesis of catalysts

I. Synthesis of catalysts

synthesis of zeolite [Ga,Al]Beta by steam-assisted dry-gel conversion (SAC)

structure of zeolite Beta (BEA)

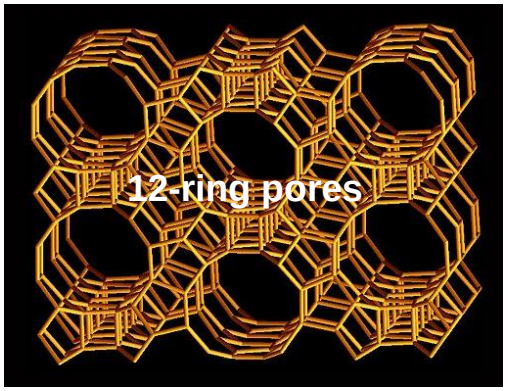

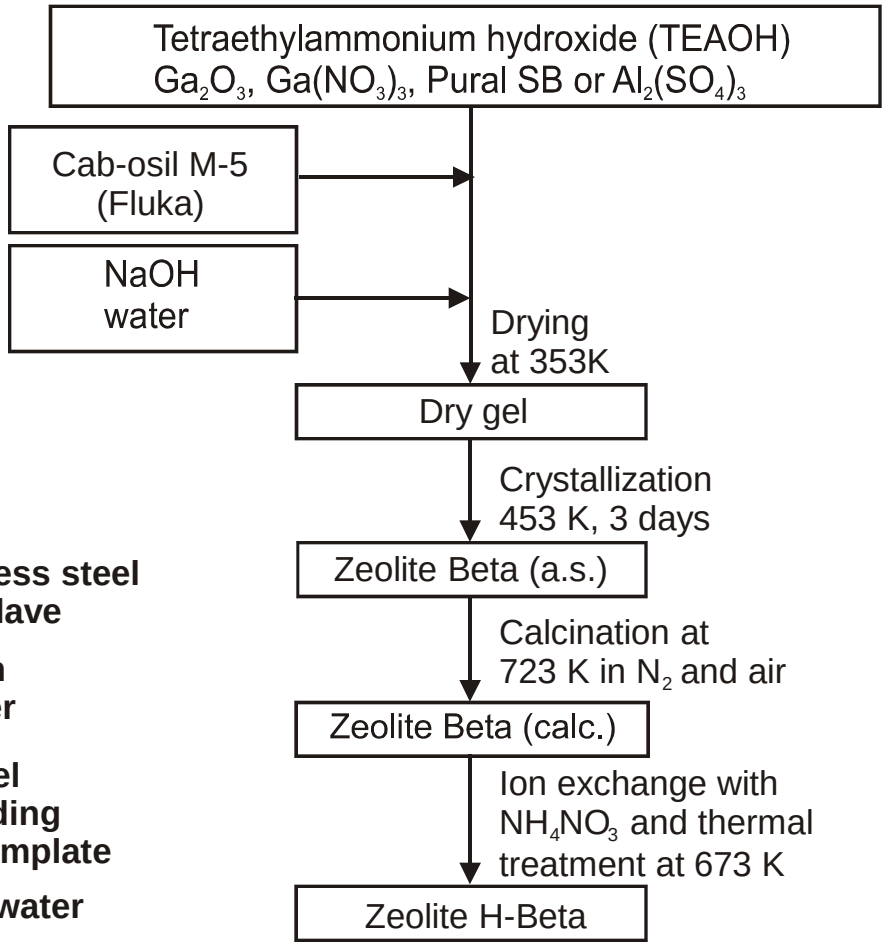

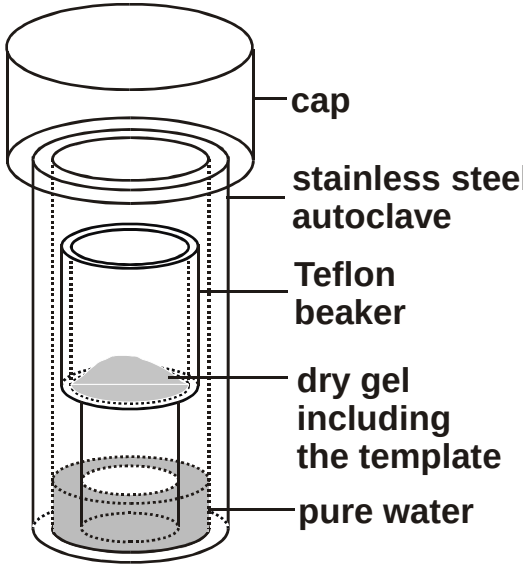

autoclave volume:
110 cm^3
Teflon beaker:
14.5 cm^3

A. Arnold et al., Microporous Mesoporous Mater. 62 (2003) 97.

I. Synthesis of catalysts

synthesis of zeolite [Ga,Al]Beta by steam-assisted dry-gel conversion (SAC)

powder X-ray diffractograms and crystallinity as a function of the dry-gel conversion time

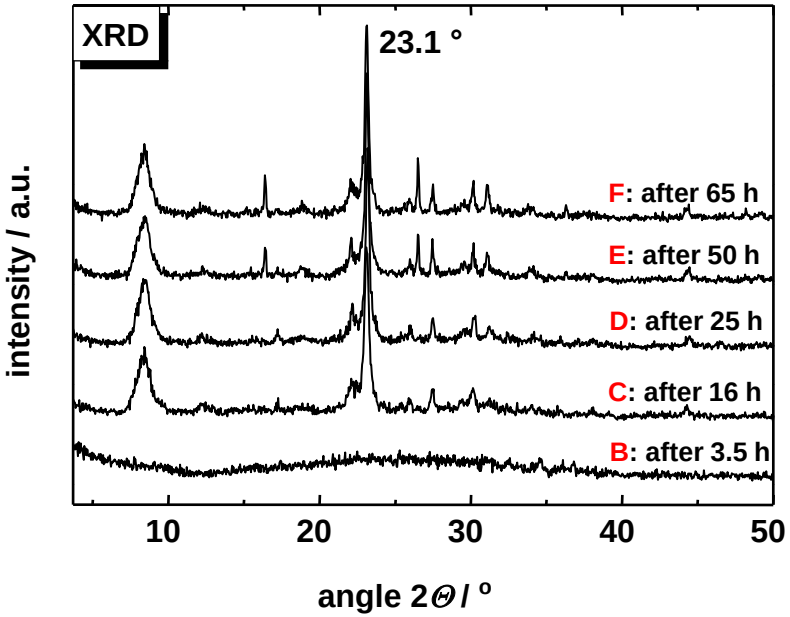

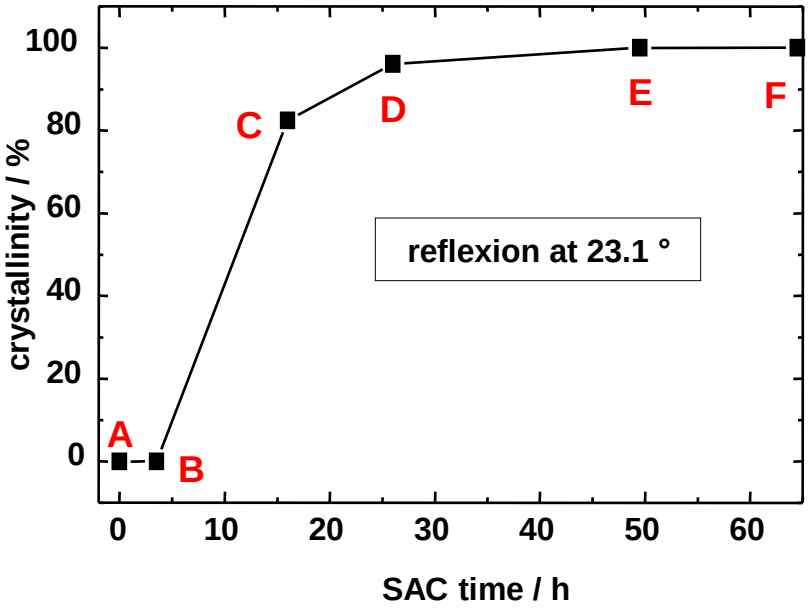

sample A: dry gel taken before conversion

samples B to F: materials taken after conversion for 3.5 to 65 h

A. Arnold et al., Microporous Mesoporous Mater. 62 (2003) 97.

I. Synthesis of catalysts

synthesis of zeolite [Ga,Al]Beta by steam-assisted dry-gel conversion (SAC)

^{29}Si MAS NMR spectra recorded after different SAC times

B_0 = 9.4 T, ν_0 = 79.5 MHz

A: fresh dry-gel particles (0 h)

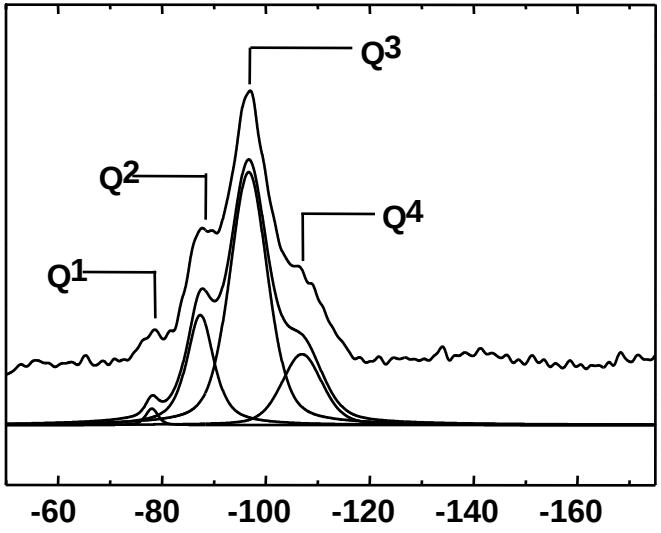

B: SAC time of 3.5 h

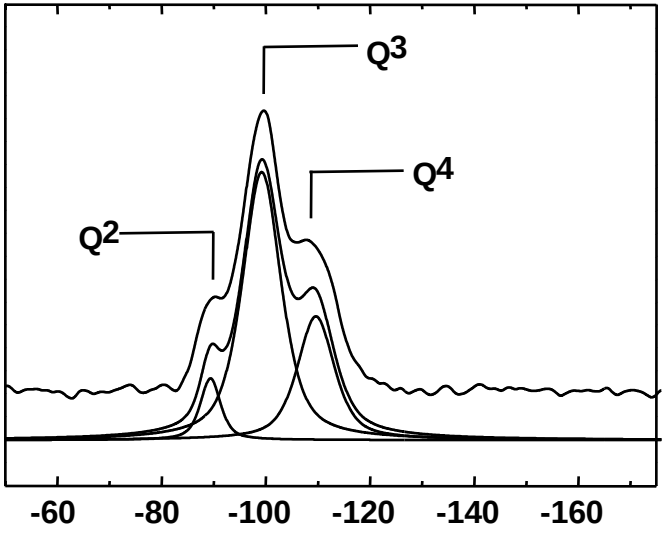

Q^1: silicon with one Si-O-Si bond, Si(1Si,3OH), at *ca.* -78 ppm

Q^4: silicon with four Si-O-Si bonds, Si(4Si), at *ca.* -107 ppm

Q^1:

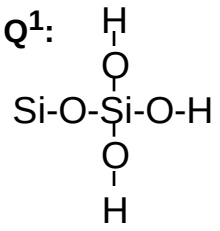

Q^4:

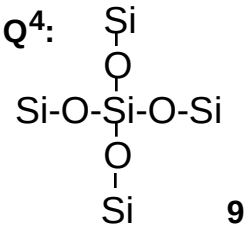

A. Arnold et al., Microporous Mesoporous Mater. 62 (2003) 97.

I. Synthesis of catalysts

synthesis of zeolite [Ga,Al]Beta by steam-assisted dry-gel conversion (SAC)

^{29}Si MAS NMR spectra recorded after different SAC times

B_0 = 9.4 T, ν_0 = 79.5 MHz

C: SAC time of 16 h

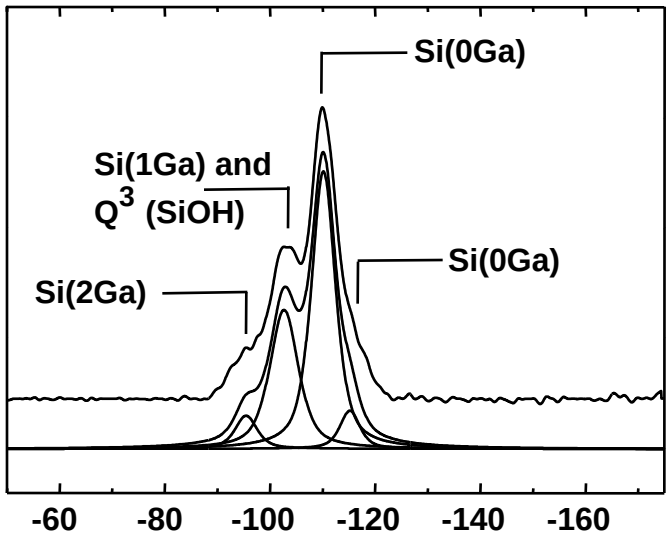

F: SAC time of 65 h

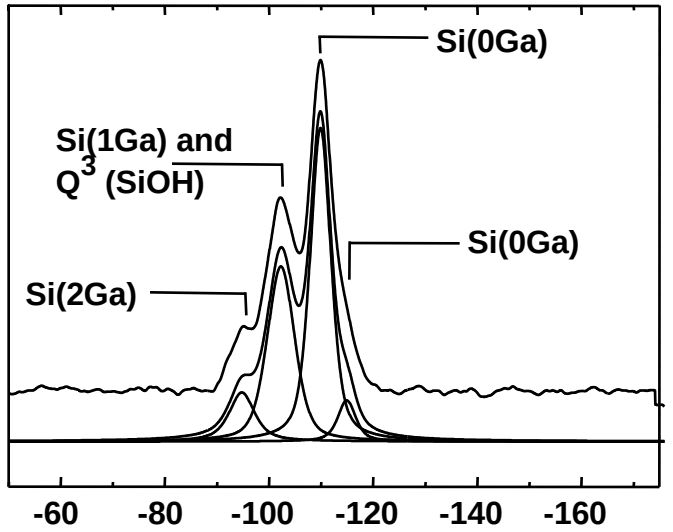

Si(1Ga): Q^4 framework silicon with one Si-O-Ga and three Si-O-Si bonds, Si(3Si,1Ga), at -101 ppm is overlapped by the Q^3 signal, Si(3Si,1OH), at *ca.* -103 ppm

Si(2Ga): framework silicon with two Si-O-Ga and two Si-O-Si bonds, Si(2Si,2Ga), at -95 ppm

Q^4: Si(3Si,1Ga)

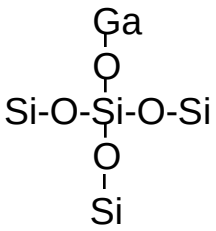

A. Arnold et al., Microporous Mesoporous Mater. 62 (2003) 97.

I. Synthesis of catalysts

synthesis of zeolite [Ga,Al]Beta by steam-assisted dry-gel conversion (SAC)

^{71}Ga MAS NMR spectra (spin *I* = 3/2) recorded after different SAC times

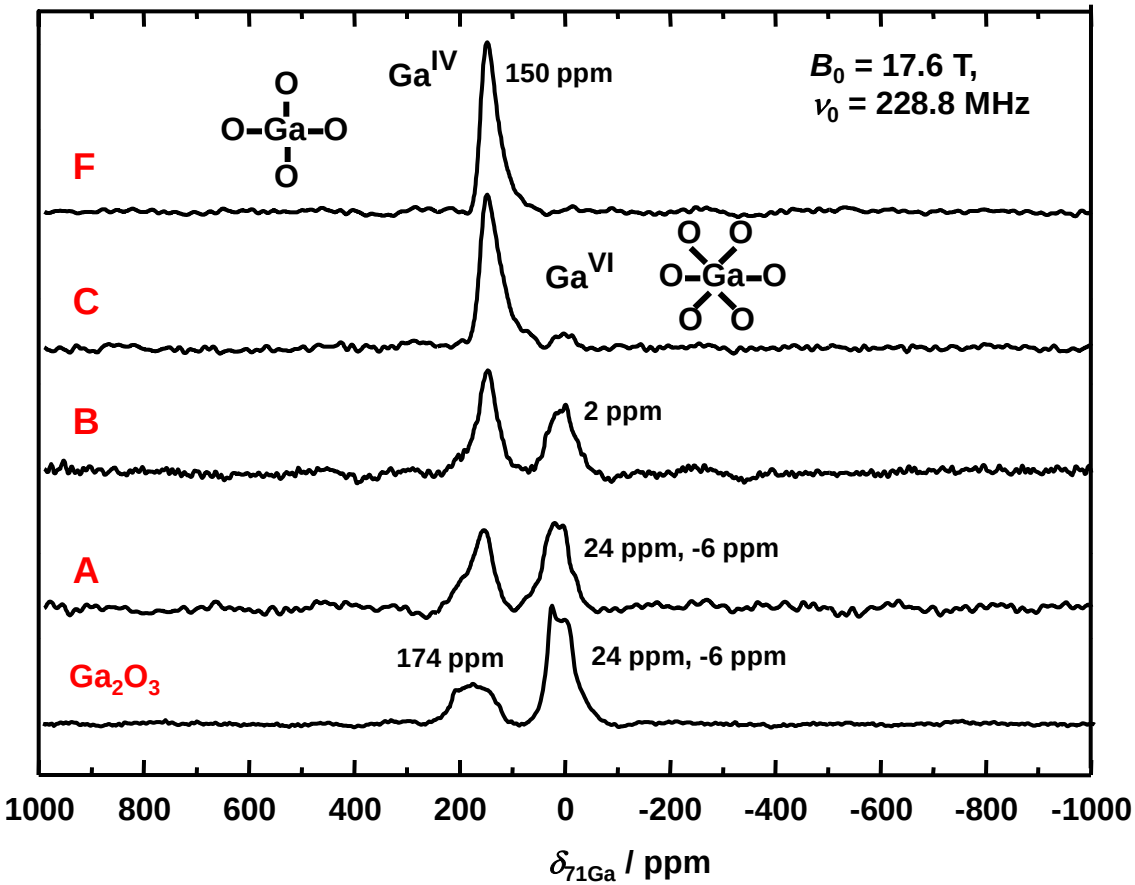

gallium coordination:

Ga^{IV} /%	Ga^{VI} /%
100	0
93	7
58	42
45	55
34	66

complete tetrahedral oxygen coordination of gallium atoms after a SAC time of 65 h

A. Arnold et al., Microporous Mesoporous Mater. 62 (2003) 97.

I. Synthesis of catalysts

synthesis of zeolite [Ga,Al]Beta by steam-assisted dry-gel conversion (SAC)

^{71}Ga MQMAS NMR spectroscopy (spin *I* = 3/2) of [Ga]Beta sample F (65 h)

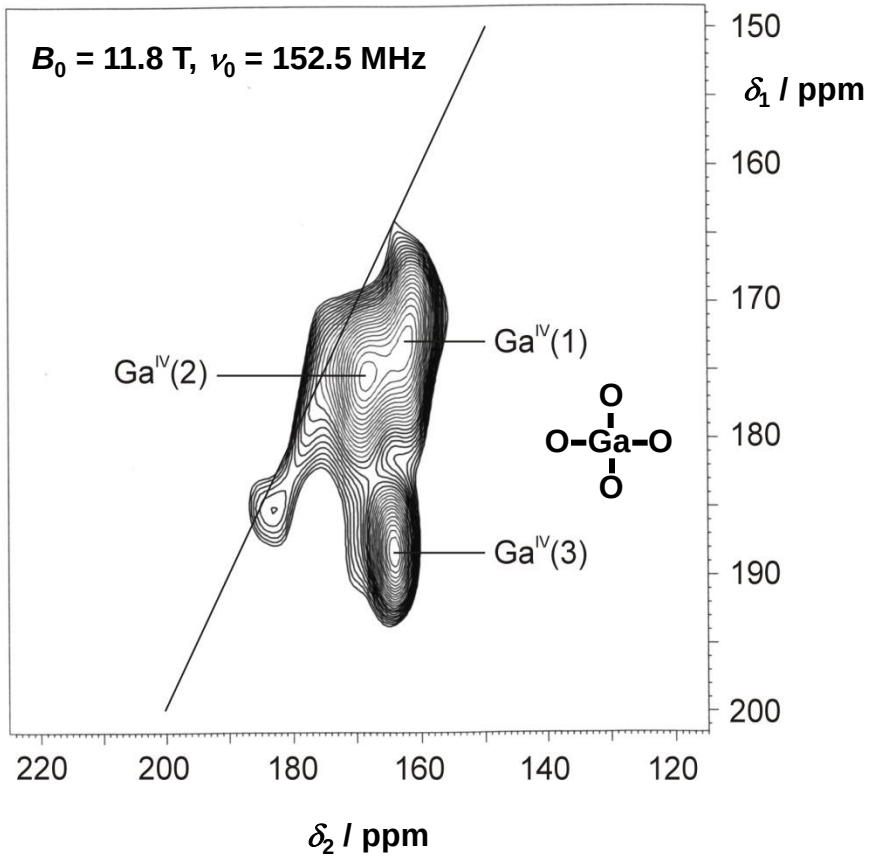

Ga^{IV}(1, 2):
framework gallium species,
SOQE = 2.2 and 1.8 MHz,
δ_{iso} = 172 and 168 ppm

Ga^{IV}(3):
extra-framework gallium species or amorphous phases,
SOQE = 4.7 MHz,
δ_{iso} = 176 ppm

***SOQE*: second-order quadrupole effect parameter, strength of quadrupolar interaction**

A. Arnold et al., Microporous Mesoporous Mater. 62 (2003) 97.

I. Synthesis of catalysts

synthesis of flame-derived silica-alumina with different aluminum contents

preparation of flame-made silica-alumina (SA) catalysts:

dissolving aluminum(III) acetylacetonate and tetraethoxysilane in a 1:1 (vol%) mixture of acetic acid and methanol

this solution was pumped through a capillary with 5 ml/min and nebulized with 5 l/min O_2

the spray was ignited by a methane/ oxygen flame (1.5/0.9 L/min) resulting in an approximately 6 cm long flame

particles (*ca.* 20 nm) were collected on a cooled Whatman GF6 filter

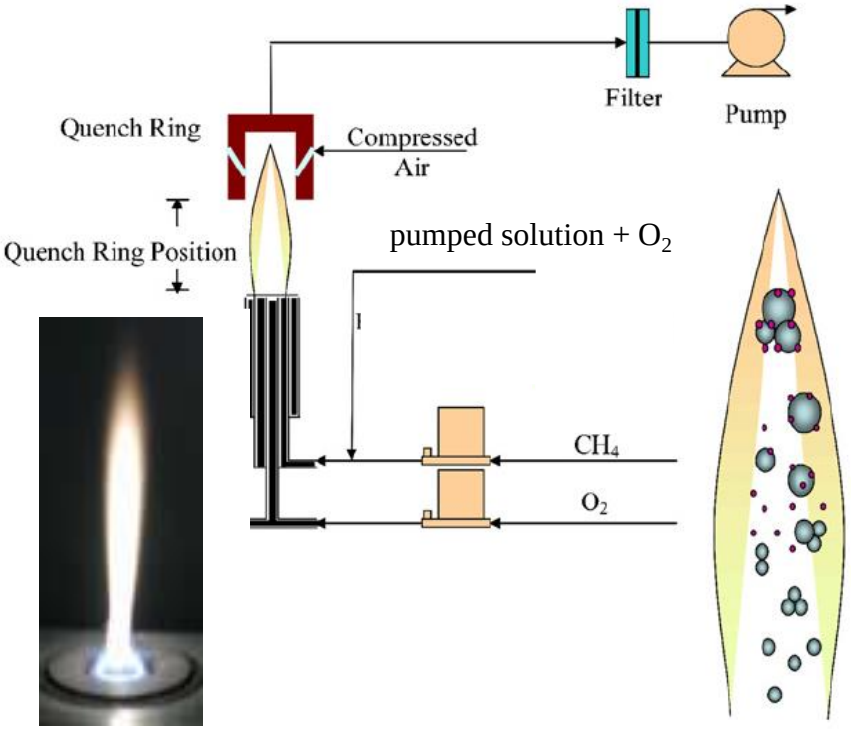

J. Huang et al., Angew. Chem. Int. Ed. 49 (2010) 7776.

I. Synthesis of catalysts

synthesis of flame-derived silica-alumina with different aluminum contents

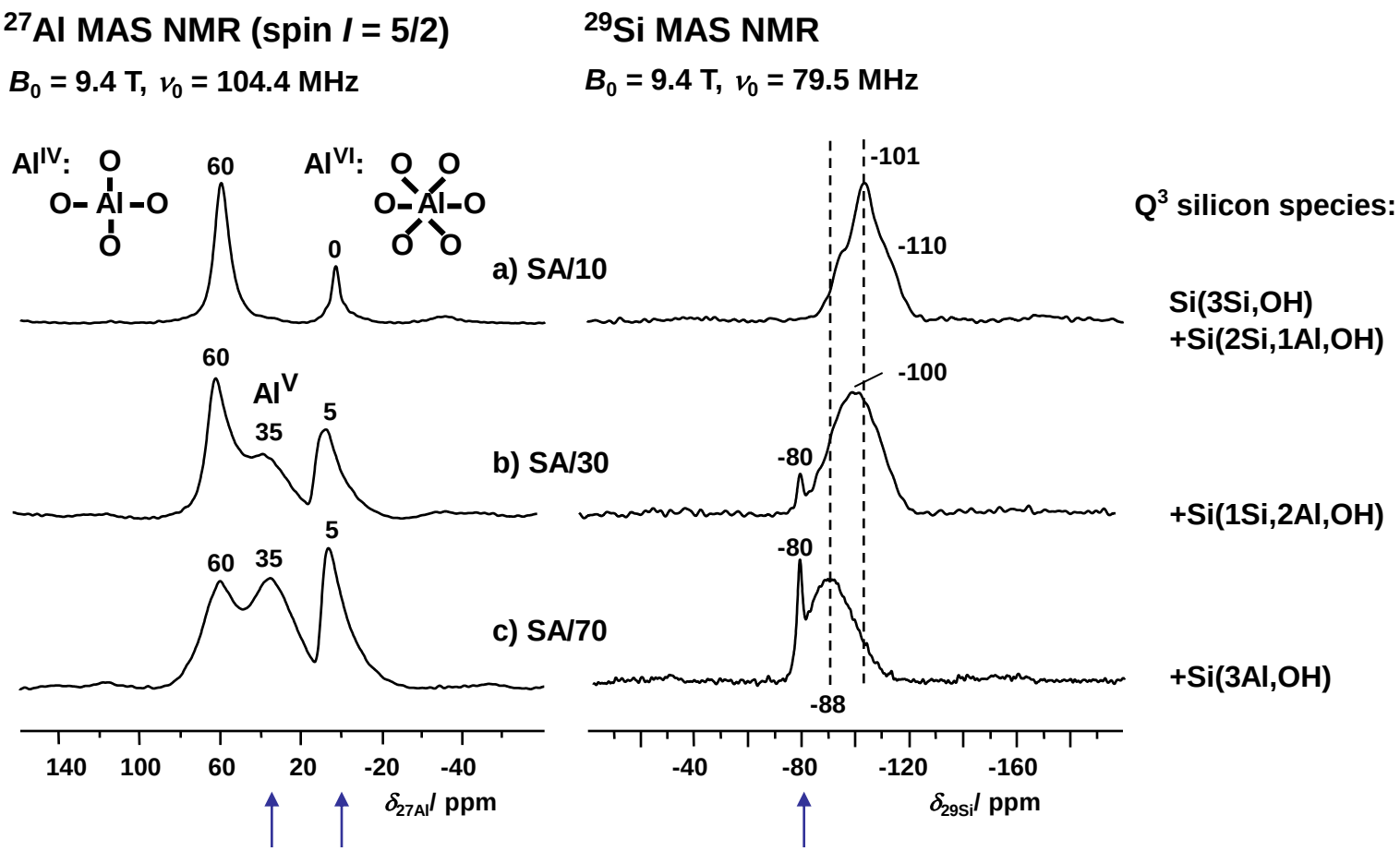

formation of andalusite phases (Al_2SiO_5) with δ_{29Si} = -79.8 ppm (M. Mägi *et al.*, J. Phys. Chem. 88 (1984) 1518) and octahedrally (δ_{27Al} = 5 ppm) as well as pentacoordinated aluminum atoms (δ_{27Al} = 35 ppm)

J. Huang et al., Angew. Chem. Int. Ed. 49 (2010) 7776.

I. Synthesis of catalysts

synthesis of flame-derived silica-alumina with different aluminum contents

^{1}H MAS NMR

upon dehydration at 723 K

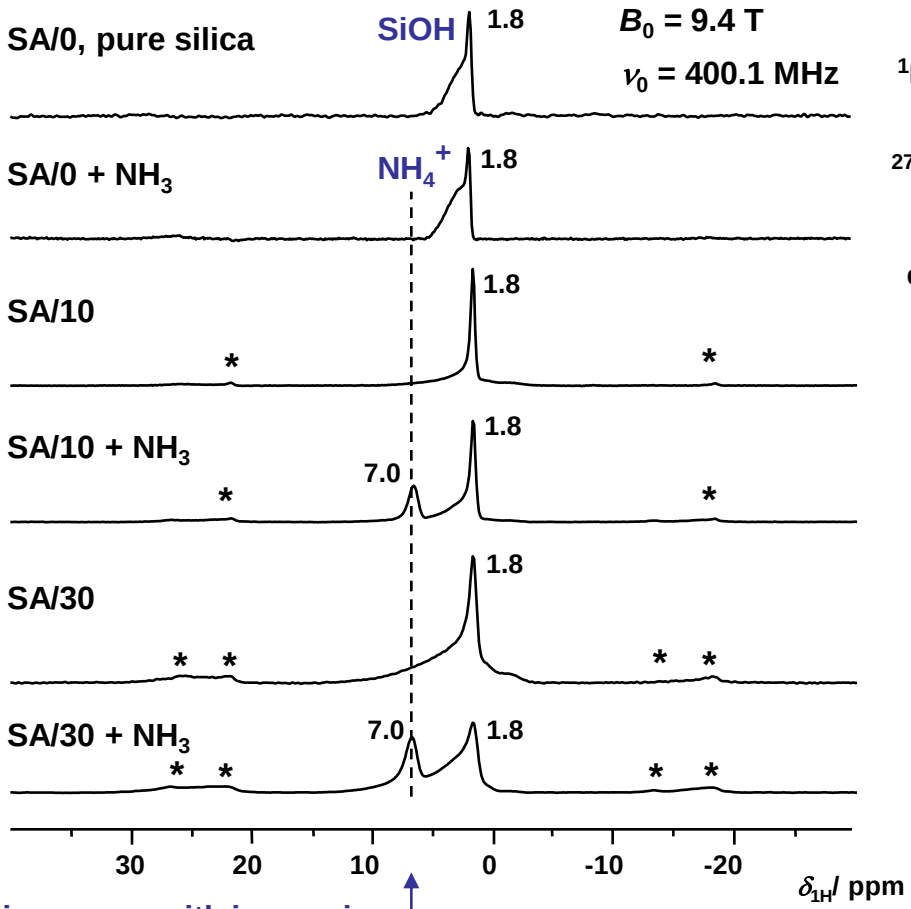

increases with increasing molar aluminum content

^{1}H/^{27}Al TRAPDOR MAS NMR

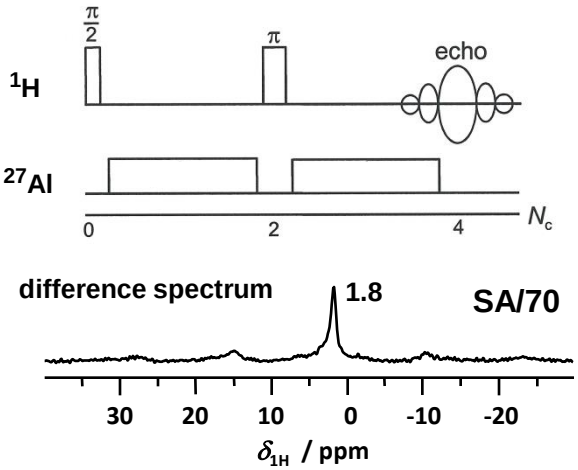

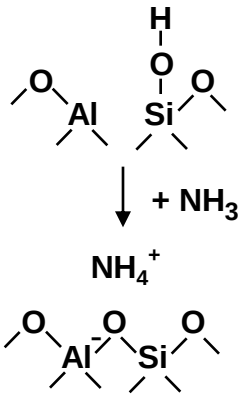

J. Huang et al., Angew. Chem. Int. Ed. 49 (2010) 7776.

II. Modification of catalysts

II. Framework modification

dealumination of zeolite H,Na-Y by steaming

structure of zeolite Y (FAU)

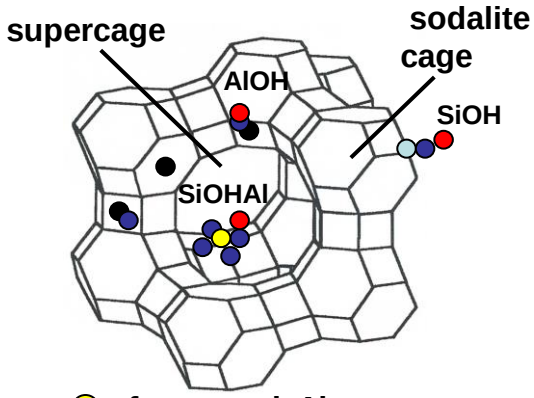

dealumination procedure

commercial zeolite Na-Y (n_{Si}/n_{Al} = 2.7) → ammonium exchange (93%) → steaming at 748 K under flowing nitrogen (100 ml/min) with a water vapor pressure of 7.4-81.5 kPa → dealuminated zeolite deH,Na-Y/31.1-81.5 (n_{Si}/n_{Al} = 3.6-6.0) → transfer into gas-tight MAS NMR rotor without rehydration

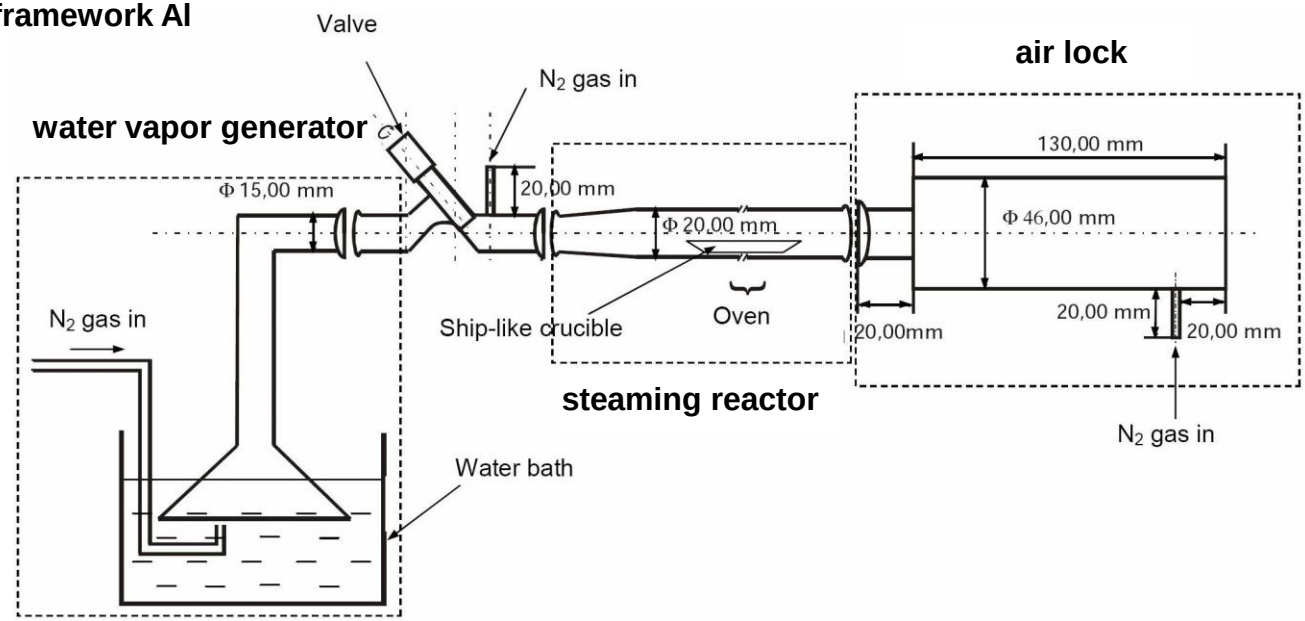

II. Framework modification

dealumination of acidic zeolites by steaming

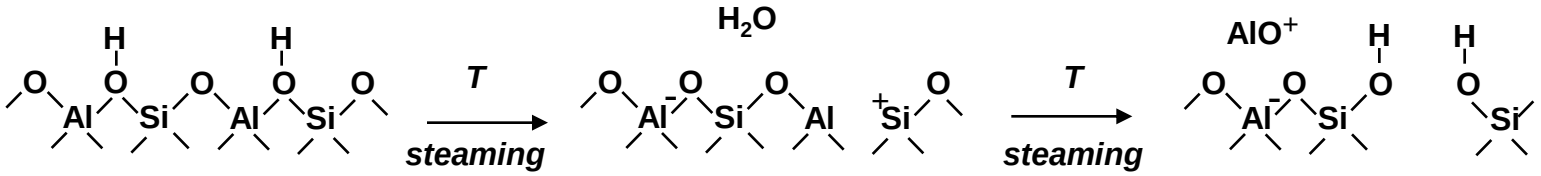

^{29}Si MAS NMR spectroscopy of zeolites H,Na-Y (left) and deH,Na-Y/31.1 (right)

B_0 = 9.4 T, ν_0 = 79.5 MHz

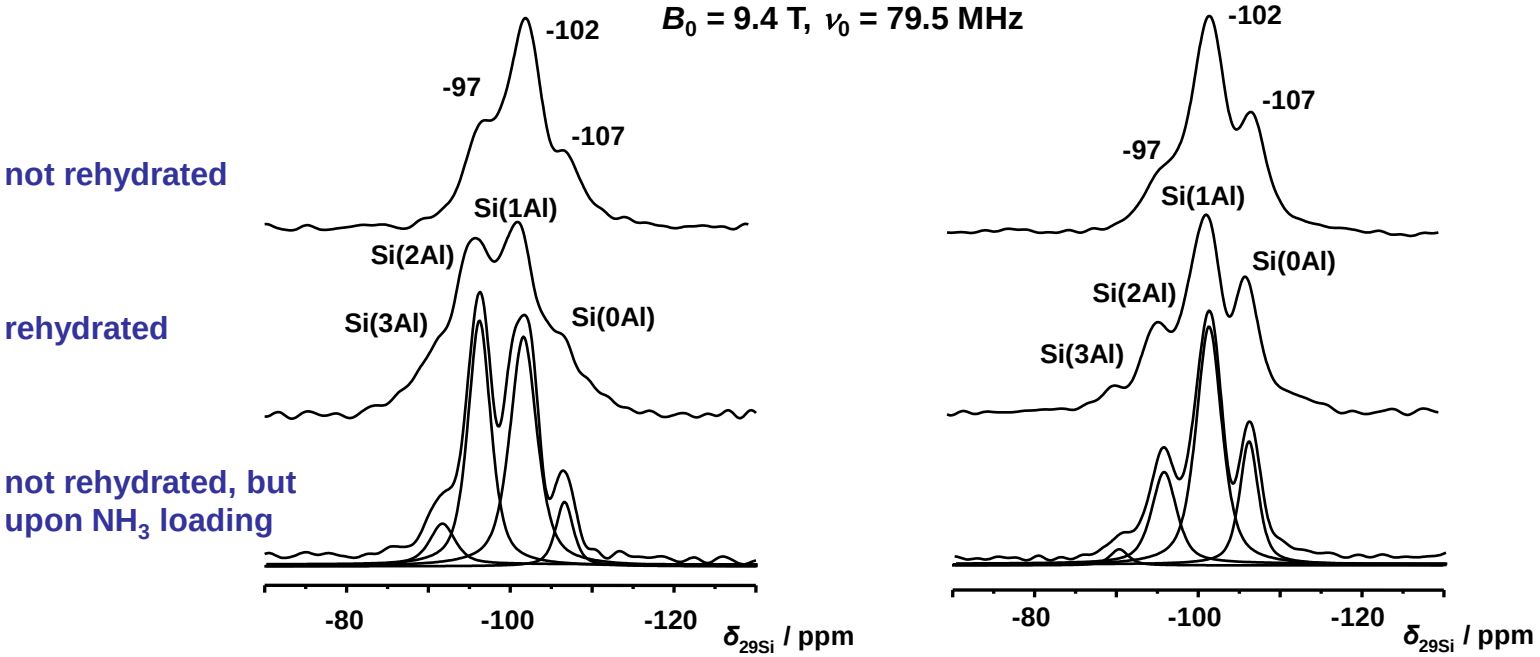

$$\frac{n_{Si}}{n_{Al}} = \frac{100}{\sum_n 0.25 \cdot n \cdot I_{Si(nAl)}}$$: 2.7 (51.9 Al^{fr} / u.c.)

3.8 (40.0 Al^{fr}/u.c + 11.9 Al^{ex}/u.c.)

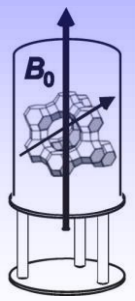

J. Jiao et al., Microporous Mesoporous Mater. 90 (2006) 246.

II. Framework modification

dealumination of zeolite H,Na-Y by steaming

^{27}Al MQMAS NMR spectroscopy (spin I = 5/2) of not rehydrated zeolite deH,Na-Y/81.5

B_0 = 17.6 T, ν_0 = 195.5 MHz, ν_{rot} = 30 kHz

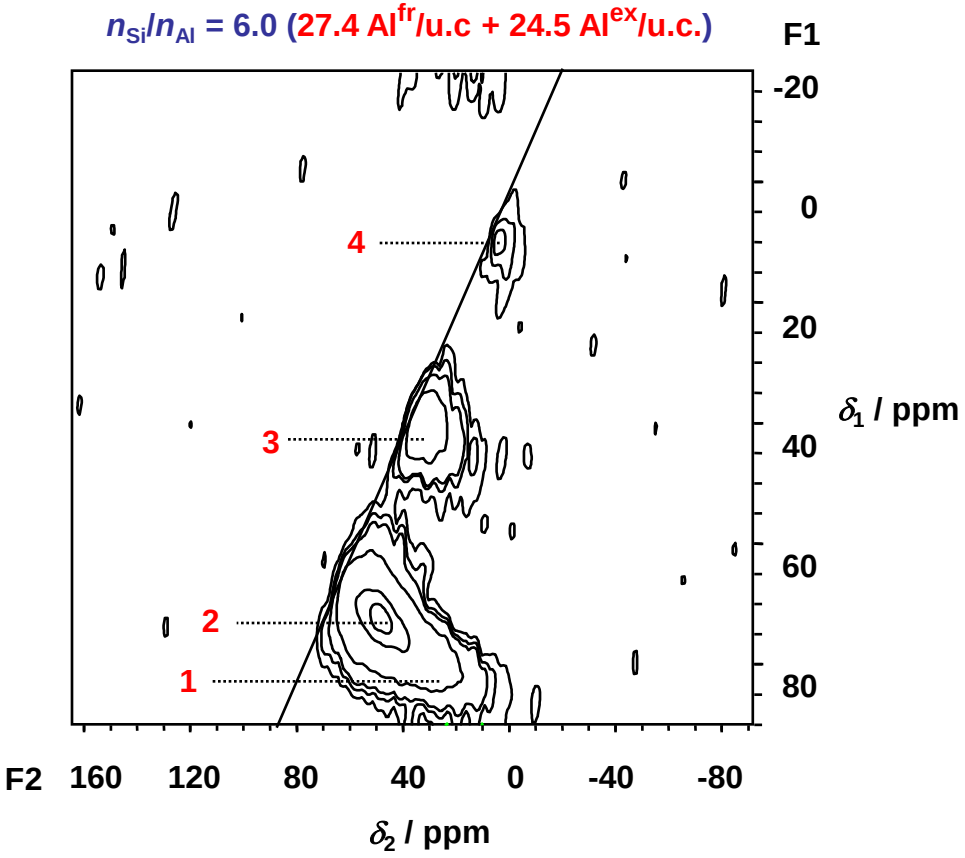

signal 1: Al^{IV}
- *SOQE* = 15.0±1.0 MHz
- δ_{iso} = 70±10 ppm

signal 2: Al^{IV}
- *SOQE* = 8.0±0.5 MHz
- δ_{iso} = 65±5 ppm

signal 3: Al^{V}
- *SOQE* = 7.5±0.5 MHz
- δ_{iso} = 35±5 ppm

signal 4: Al^{VI}
- *SOQE* = 5.0±0.5 MHz
- δ_{iso} = 10±5 ppm

J. Jiao et al., Phys. Chem. Chem. Phys. 7 (2005) 3221.

II. Framework modification

dealumination of zeolite H,Na-Y by steaming

^{27}Al solid-state NMR spectroscopy (spin I = 5/2) of zeolite deH,Na-Y/81.5 (51.9 Al/u.c.)

B_0 = 17.6 T, ν_0 = 195.5 MHz

^{27}Al spin-echo NMR

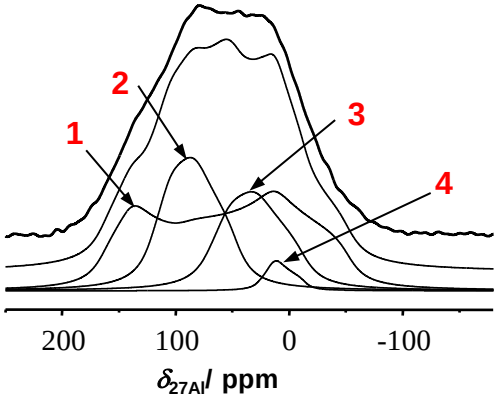

^{27}Al MAS NMR ν_{rot} = 30 kHz

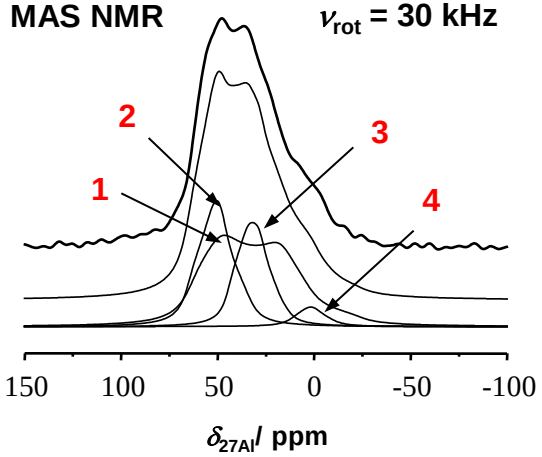

Signals	1	2	3	4
assignments	Al^{IV}/H^+ $Al^{IV}/Al^{cat,x+}$	Al^{IV}/Na^+ cluster Al^{IV}	$Al^{V,x+}$ cat.	cluster Al^{VI}
δ_{iso} / ppm	70±10	65±5	35±5	10±5
C_{QCC} / MHz	15.0±1.0	8.0±0.5	7.5±0.5	5.0±0.5
η_Q	0.3	0.8	0.7	0.7
I in %	48 (27+21)	27 (7+20)	21	4

extra-framework Al cations ($Al^{V,x+}$):

10.9 $Al^{V,x+}$/u.c.

extra-framework Al_2O_3 clusters:

12.5 $Al^{cluster}$/u.c.

in comparison with 24.5 Al^{ex}/u.c. calculated using results of ^{29}Si MAS NMR spectroscopy

J. Jiao et al., Phys. Chem. Chem. Phys. 7 (2005) 3221.

II. Modification of catalysts

VPO catalysts supported on mesoporous SBA-15 materials

selective oxidation of *n*-butane

Mars van Krevelen mechanism

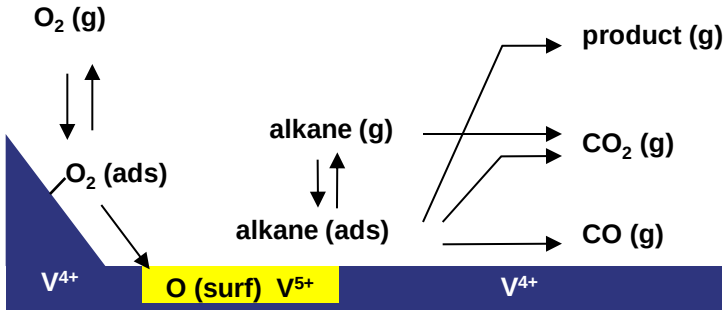

discussed phase transitions

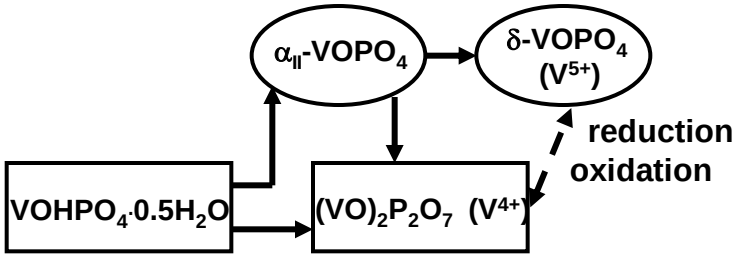

preparation procedure of X.-K. Li et al., J. Catal. 238 (2006) 232:

- siliceous SBA-15 is added to isobutyl/benzyl alcohols (1 : 1) with V_2O_5 and H_3PO_4
- activation in a flow of 1.5 % *n*-butane, 17.5 % O_2 and balance N_2 (100 ml/min) at 673 K

II. Framework modification

VPO catalysts supported on mesoporous SBA-15 materials

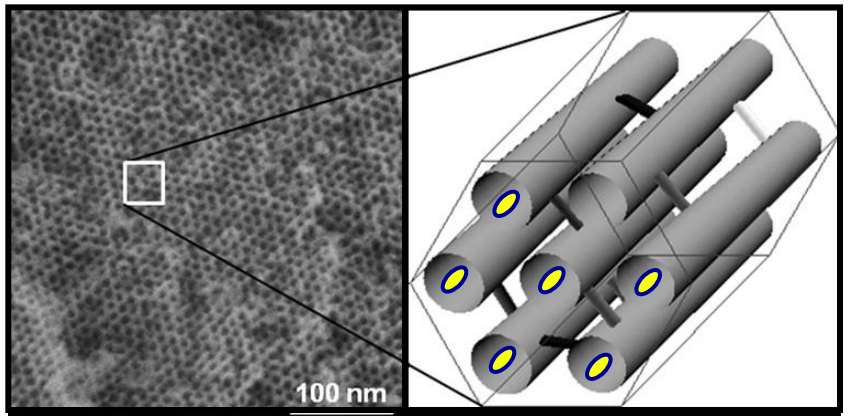

Materials	P / V	BET surface m^2 / g	Pore volume cm^3 / g
SBA-15	-	1164	1.25
20%VPO/SBA-15	1.09	662	0.80
60%VPO/SBA-15	1.04	456	0.54

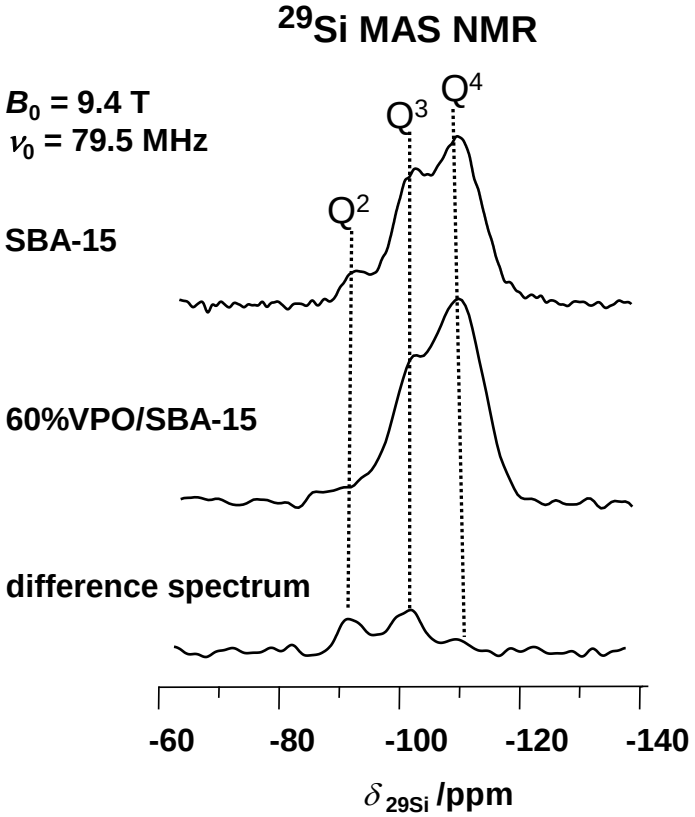

VPO is bound at former silanol groups on the mesoporous surface of SBA-15

J. Frey et al., Solid State Nucl. Magn. Reson. 35 (2009) 130

II. Framework modification

VPO catalysts supported on mesoporous SBA-15 materials

^{51}V MAS NMR spectroscopy (spin I = 7/2) of 60%VPO/SBA-15 after activation

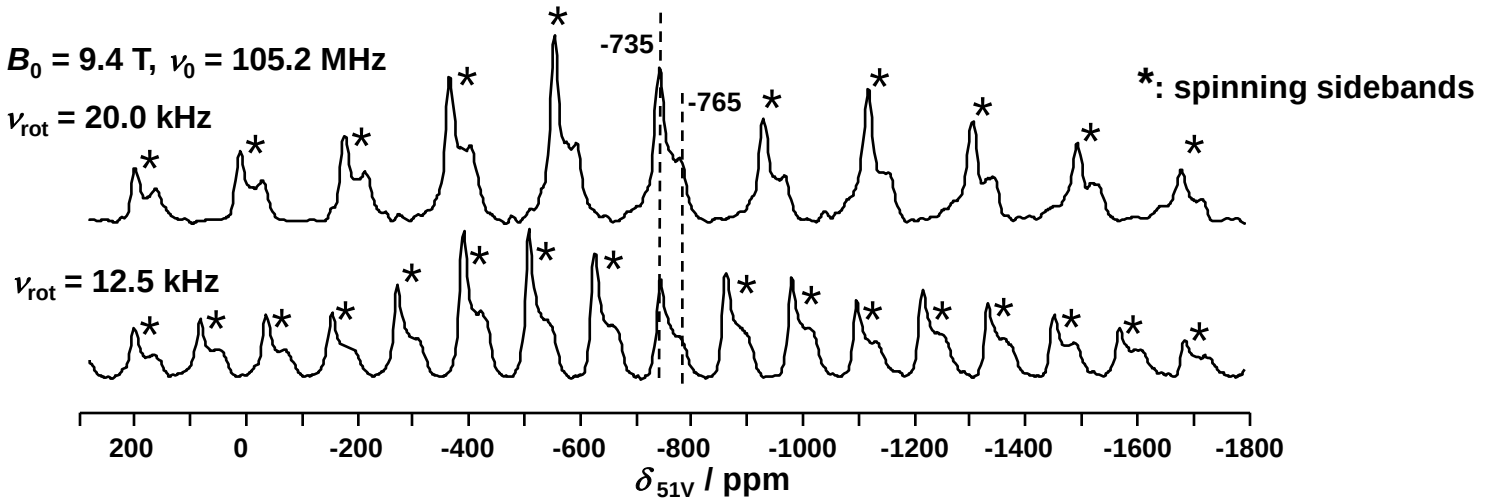

Materials	δ_{iso} / ppm	$\Delta\sigma_{CSA}$ / ppm	η_{CSA}	C_Q / MHz	η_Q
60%VPO/SBA-15	-735 -765	900 950	0.10 0.10	2.00 1.90	0.60 0.60
α_{II}-$VOPO_4$ [1)]	-755	992	0.08	0.63	0.09
β-$VOPO_4$ [1)]	-735	818	0.05	1.45	0.44

[1)] R. Siegel et al., Mag. Res. Chem. 42 (2004) 1022.
O.B. Lapina et al., Prog. Nucl. Magn. Reson. Spetrosc. 53 (2008) 128.

J. Frey et al., Solid State Nucl. Magn. Reson. 35 (2009) 130

II. Framework modification

VPO catalysts supported on mesoporous SBA-15 materials

^{31}P MAS NMR spectroscopy of 60%VPO/SBA-15 before and after activation

B_0 = 9.4 T
ν_0 = 162.0 MHz
ν_{rot} = 10 kHz

non-activated precursor

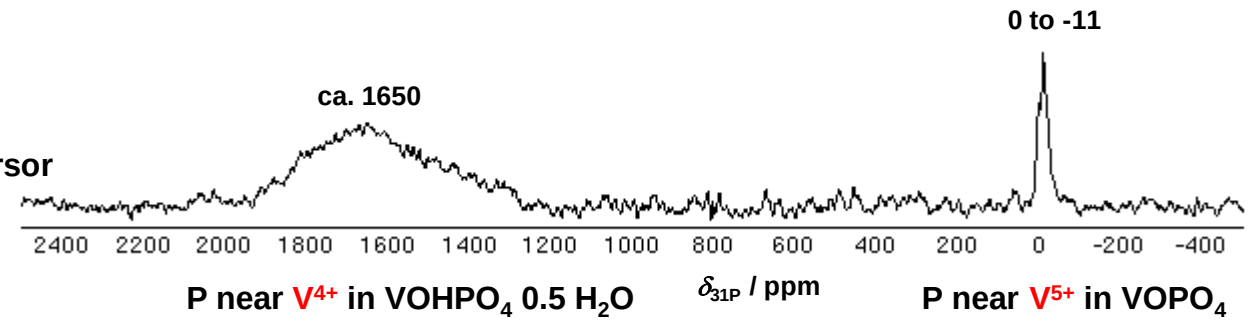

activated at 673 K for 15 h

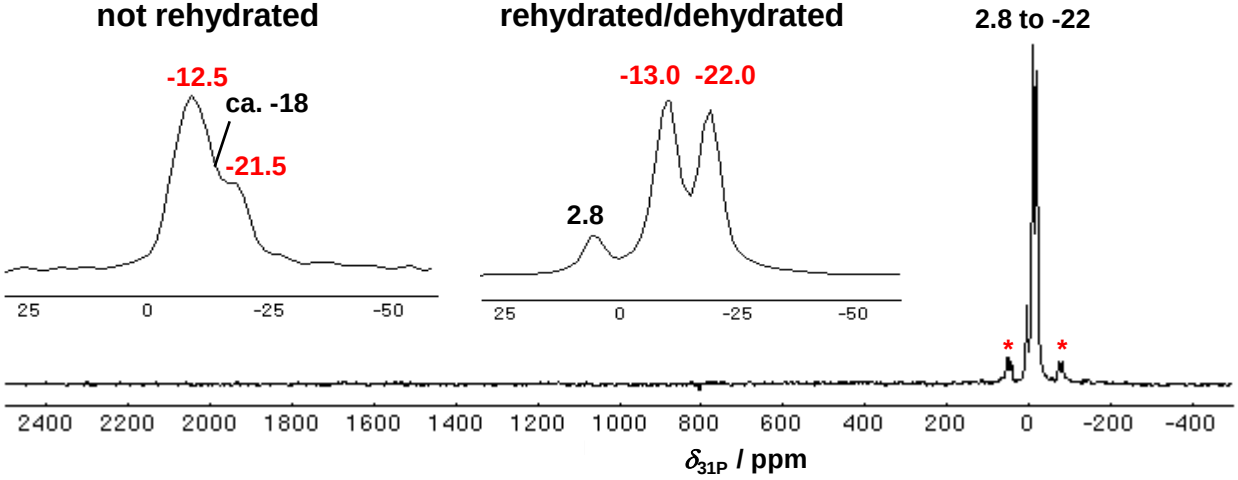

P near V^{5+} in $VOPO_4$ phases, such as β-$VOPO_4$ (-13 ppm) and α_{II}-$VOPO_4$ (-22 ppm)

J. Frey et al., Solid State Nucl. Magn. Reson. 35 (2009) 130

II. Framework modification

VPO catalysts supported on mesoporous SBA-15 materials

selective oxidation of *n*-butane to maleic anhydride at 678 K with sequential switching on (15 min) and off (40 min) of the gaseous oxygen

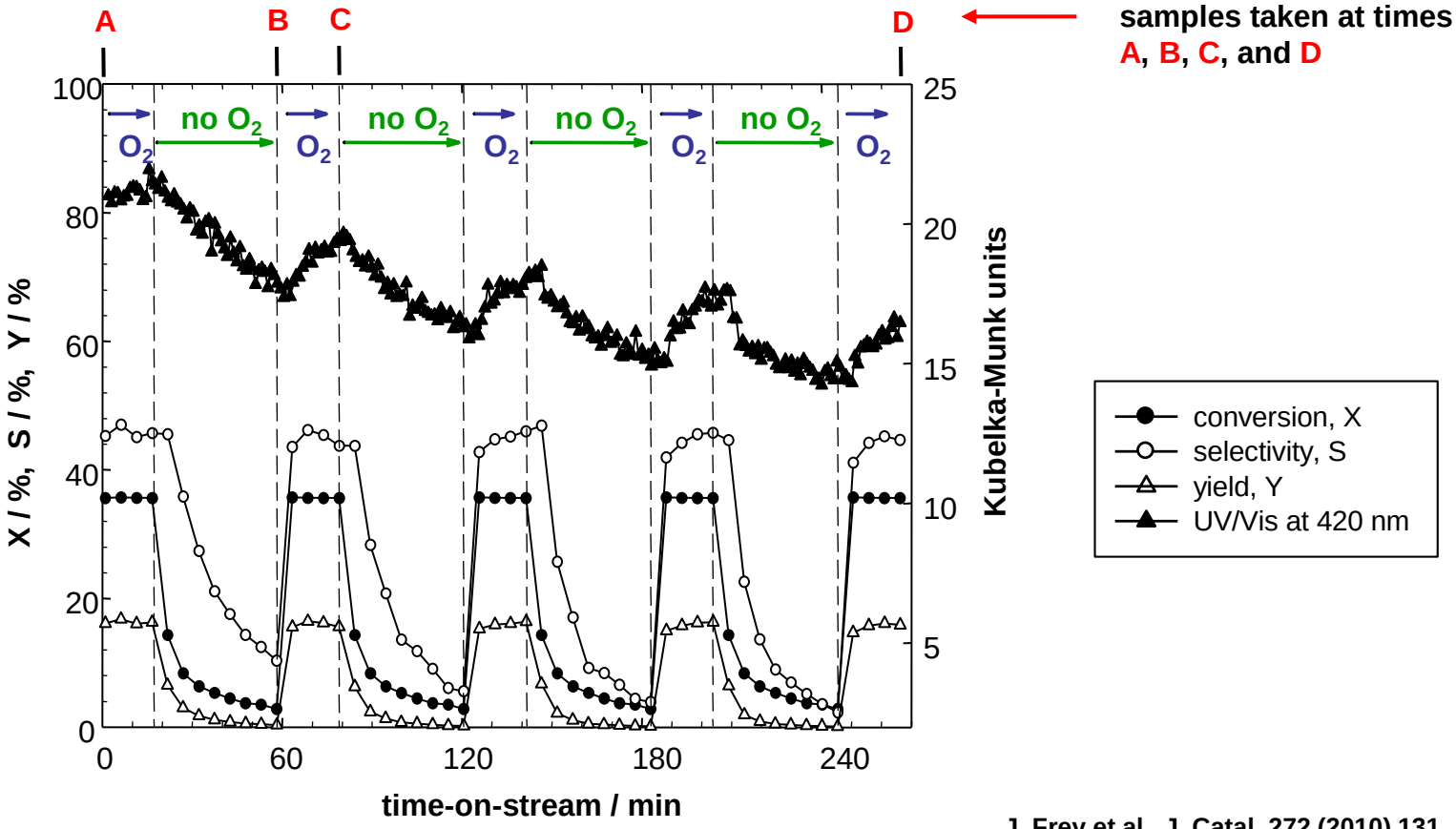

J. Frey et al., J. Catal. 272 (2010) 131

II. Framework modification

VPO catalysts supported on mesoporous SBA-15 materials

^{31}P MAS NMR spectra of VPO/SBA-15/A to VPO/SBA-15/D

B_0 = 9.4 T, ν_0 = 162.0 MHz

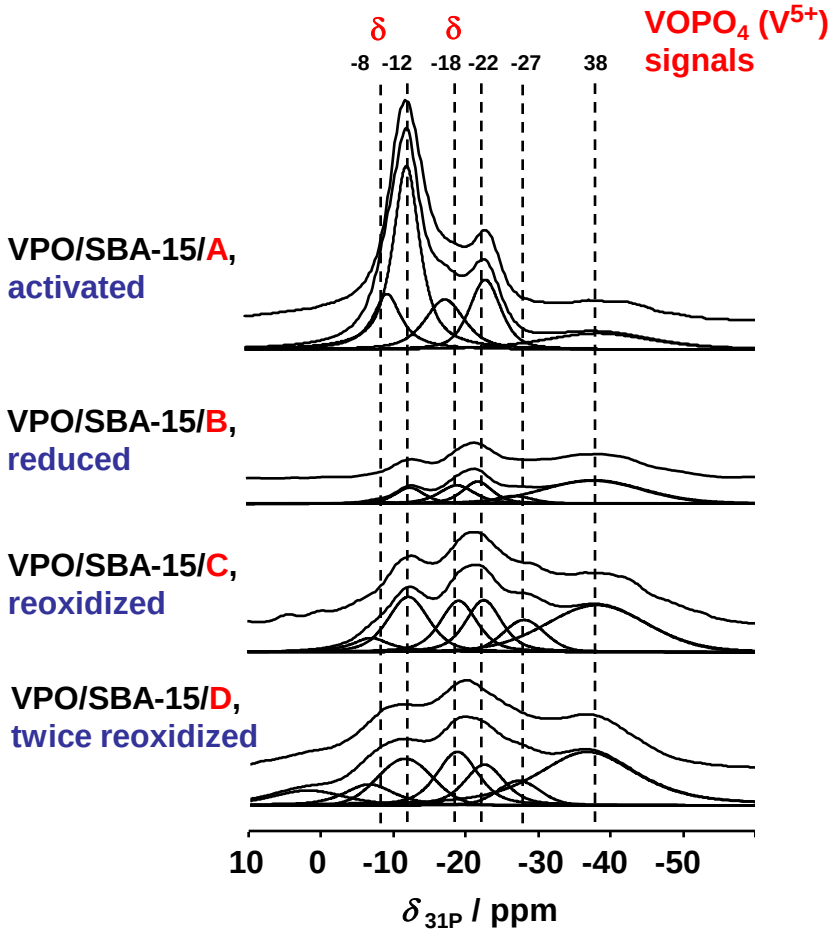

Catalysts	Samples	Contents of P/V^{5+}
VPO/bulk	A	0.5 %
	B	0 %
	C	0.35 %
	D	0.4 %
VPO/SBA-15	A	2.6 %
	B	0.3 %
	C	0.9 %
	D	1.3 %

J. Frey et al., J. Catal. 272 (2010) 131.

III. Tailoring of surface sites

III. Tailoring of surface sites

nature of acid sites on zeolites

zeolite Y (FAU, faujasite): supercages connected via 12-ring windows (0.74 nm)

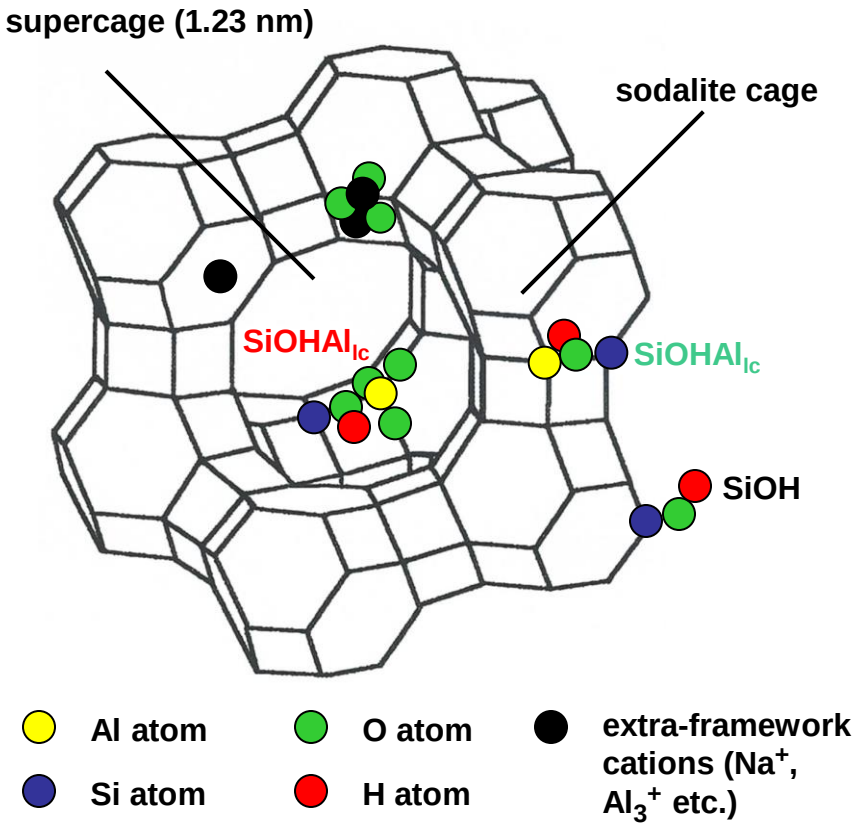

Brønsted acid sites:

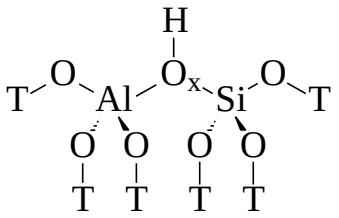

bridging OH group (SiOHAl)

Lewis acid sites:

- framework defects,
- extra-framework species (Al oxide clusters)

III. Tailoring of surface sites

preparation of dehydrated catalyst samples

vacuum line for dehydration of catalyst samples in glass tubes at elevated temperatures (often 673 K)

transfer of the dehydrated catalyst samples from glass tubes into MAS rotors inside a glove box (dry nitrogen)

III. Tailoring of surface sites

modification of Brønsted acid sites in zeolites *via* steaming

^{1}H MAS NMR

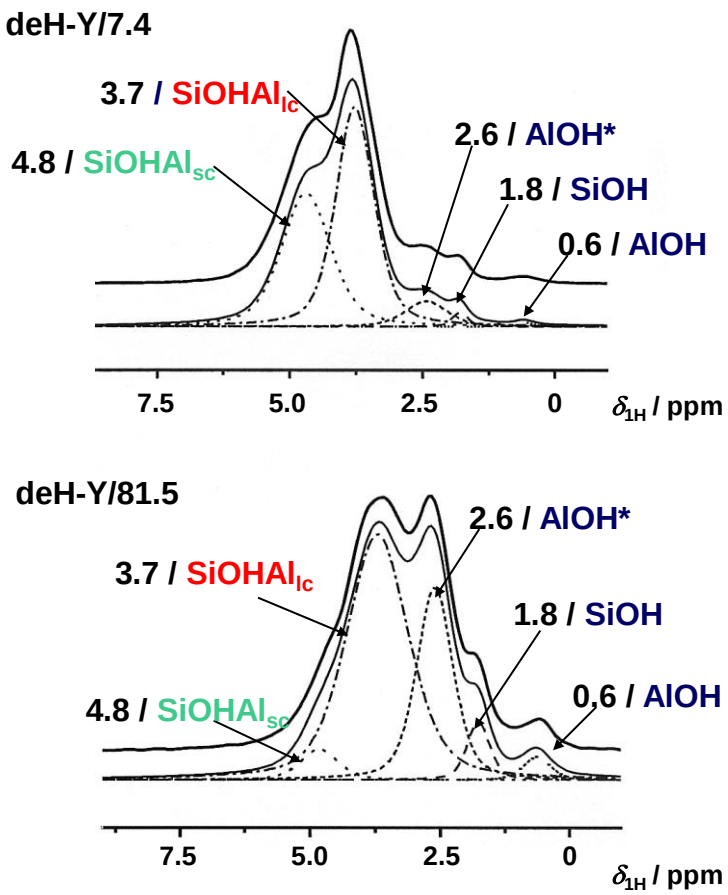

undisturbed metal OH (AlOH) groups:
-0.5 to 0.5 ppm

defect SiOH groups:
1.2 to 2.2 ppm

AlOH* groups at extra-framework Al clusters:
2.8 to 3.6 ppm

bridging OH groups in large cages and pores (SiOHAl$_{lc}$):
3.6 to 4.3 ppm

bridging OH groups in small cages (SiOHAl$_{sc}$):
4.6 to 5.2 ppm

(hydrogen bonded SiOH and SiOHAl groups: 5.2 to 13 ppm)

J. Jiao et al., J. Phys. Chem B. 108 (2004) 14305.

III. Tailoring of surface sites

preparation of Brønsted acid sites in zeolites *via* exchange with multivalent cations

exchange of zeolite Na-Y (n_{Si}/n_{Al} = 2.7) in 0.1 M $Al(NO_3)_3$ solution

Hirschler Plank mechanism

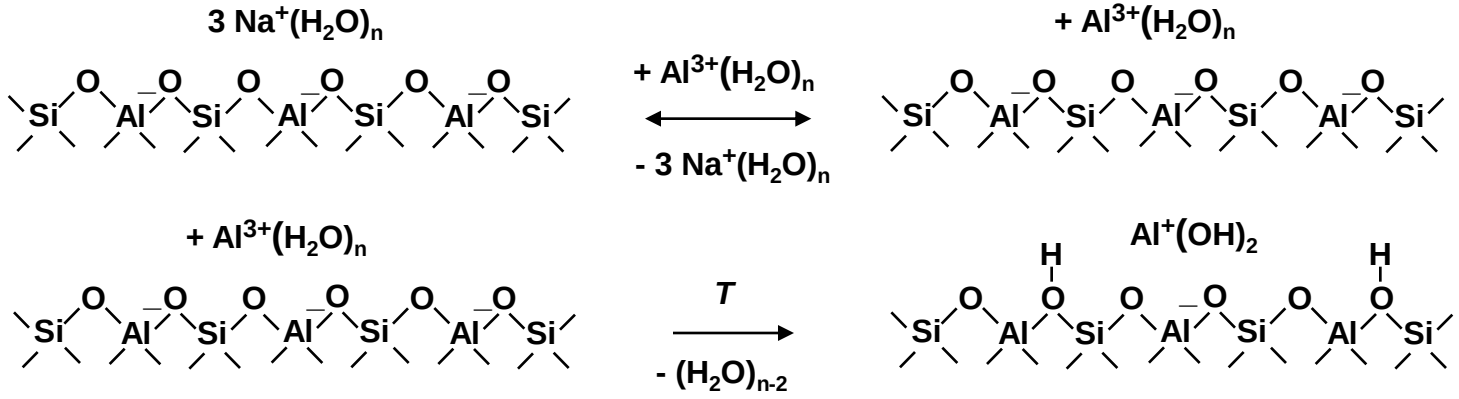

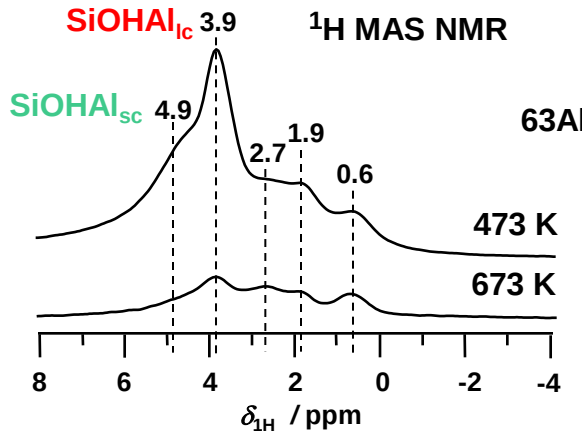

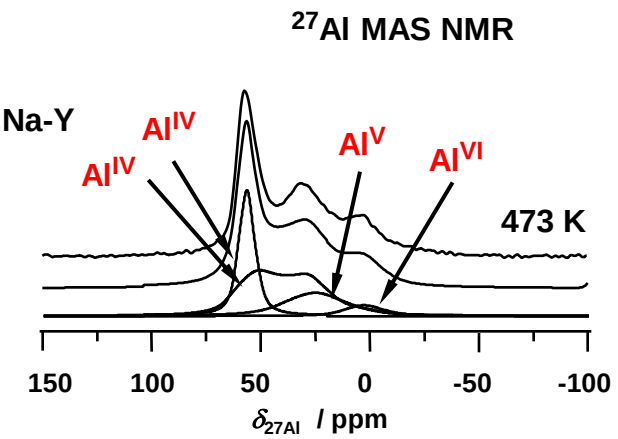

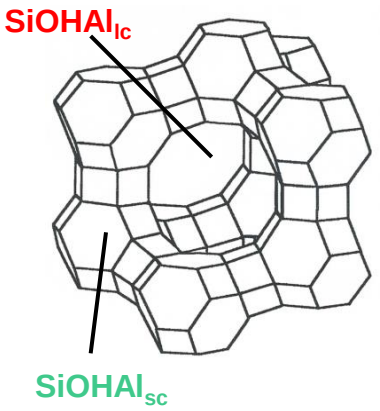

J. Huang et al., J. Phys. Chem. C 112 (2008) 3811.

III. Tailoring of surface sites

preparation of Brønsted acid sites in zeolites *via* exchange with multivalent cations

^{27}Al MQMAS NMR (spin I = 3/2)

B_0 = 17.6 T, ν_0 = 195.5 MHz, ν_{rot} = 30 kHz

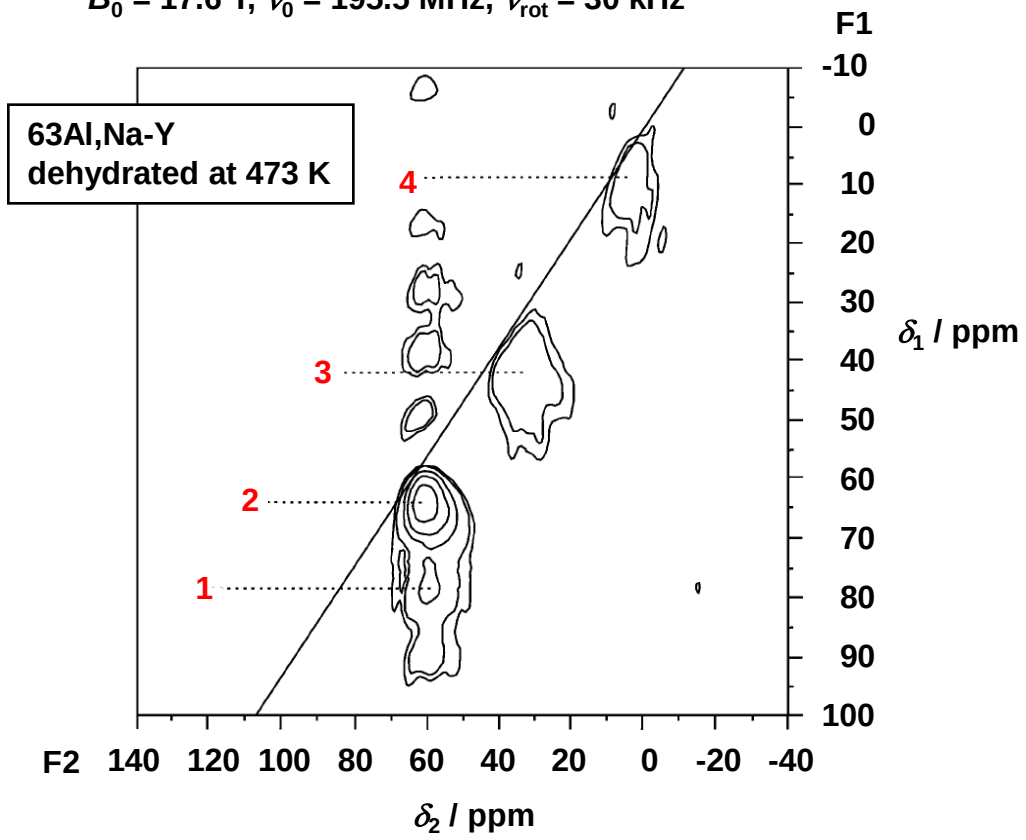

signal 1: Al^{IV}
- *SOQE* = 10.1 MHz
- δ_{iso} = 71 ppm

signal 2: Al^{IV}
- *SOQE* = 3.6 MHz
- δ_{iso} = 62 ppm

signal 3: Al^{V}
- *SOQE* = 7.6 MHz
- δ_{iso} = 39 ppm

signal 4: Al^{VI}
- *SOQE* = 6.2 MHz
- δ_{iso} = 6 ppm

J. Huang et al., J. Phys. Chem. C 112 (2008) 3811.

III. Tailoring of surface sites

Brønsted acid sites in zeolites prepared via exchange with multivalent cations (Al^{3+})

determination of the concentration of OH groups by evaluation of the ^{1}H MAS NMR intensities

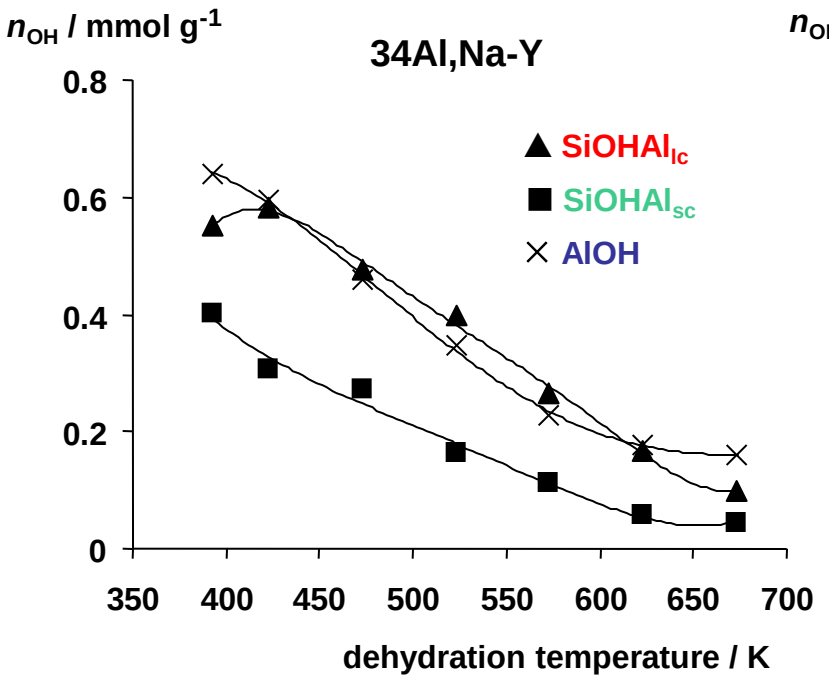

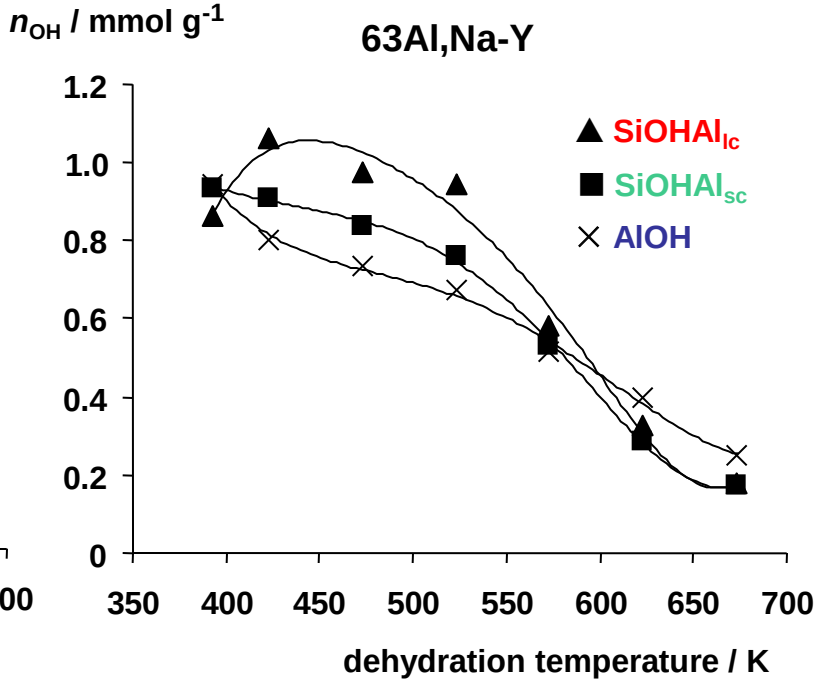

cation-exchange degree and dehydration temperature affect the number of Brønsted sites

J. Huang et al., J. Phys. Chem. C 112 (2008) 3811.

III. Tailoring of surface sites

characterization of the Brønsted acid strength *via* acetonitrile-induced low-field shift $\Delta\delta_{1H}$

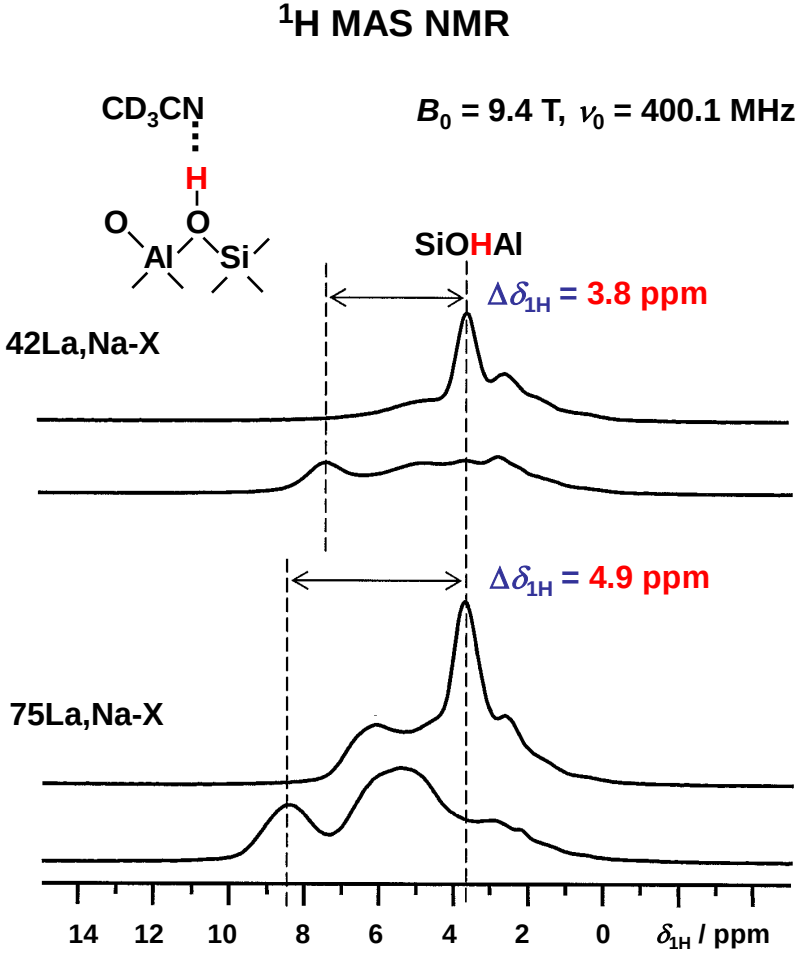

Low-field shift $\Delta\delta_{1H}$	Adsorbent and type of OH group
1.2 ppm	AlOH in MIL-53(Al)
3.6 ppm	H,Na-X (Si/Al= 1.3)
3.8 ppm	42La,Na-X and 32Al,Na-X (Si/Al = 1.4)
4.9 ppm	75La,Na-X (S/Al = 1.4)
5.1 ppm	H,Na-Y (Si/Al = 2.7)
5.3 ppm	34Al,Na-Y and 63Al,Na-Y (Si/Al = 2.7)
5.7 ppm	42La,Na-Y and 75La,Na-Y (Si/Al = 2.7)
6.5 ppm	steamed deH,Na-Y/81.5 (Si/Al = 6)
6.7 ppm	H-MOR (Si/Al = 10)
7.0 ppm	dealuminated H,Na-Y (Si/Al = 18)
7.9 ppm	H-ZSM-5 (Si/Al = 26)

Y. Jiang et al., Solid State Nucl. Magn. Reson. 39 (2011) 116-141.

III. Tailoring of surface sites

characterization of Brønsted and Lewis acid sites *via* ^{13}C-2-acetone as probe molecule

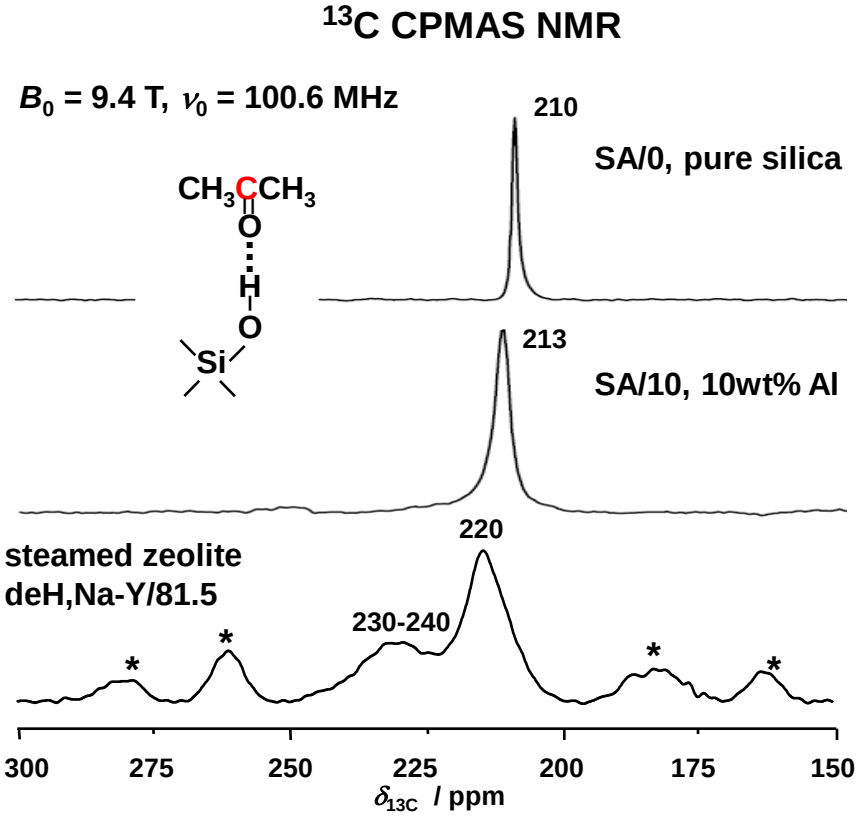

Materials	δ_{13C}	δ_{13C}
$CDCl_3$	205 ppm	0 ppm
SA/0	210 ppm	5 ppm
SA/10	213 ppm	8 ppm
H,Na-X	215 ppm	10 ppm
SA/70	216 ppm	11 ppm
H,Na-Y	220 ppm	15 ppm
ZSM-5	223 ppm	18 ppm
Lewis sites	230-240 ppm	25-35 ppm

J.F. Haw et al., Accounts of Chemical Research 29 (1996) 259.

Lewis sites formed by steaming

Brønsted sites with different acid strengths (see Tab.)

Y. Jiang et al., Solid State Nucl. Magn. Reson. 39 (2011) 116-141.
H. Fang et al., J. Phys. Chem. C 114 (2010) 12711-12718.

III. Tailoring of surface sites

comparison of different acidity scales

acids under study	$CDCl_3$ HX		HY HZSM-5		H_2SO_4(100%) $AlCl_3$	SO_3/H_2SO_4(30%)	FSO_3H/SbF_5 (4:1)	SbF_5
δ_{13C} of acetone-2-^{13}C	205	215	220	223	244	245	246	248	250

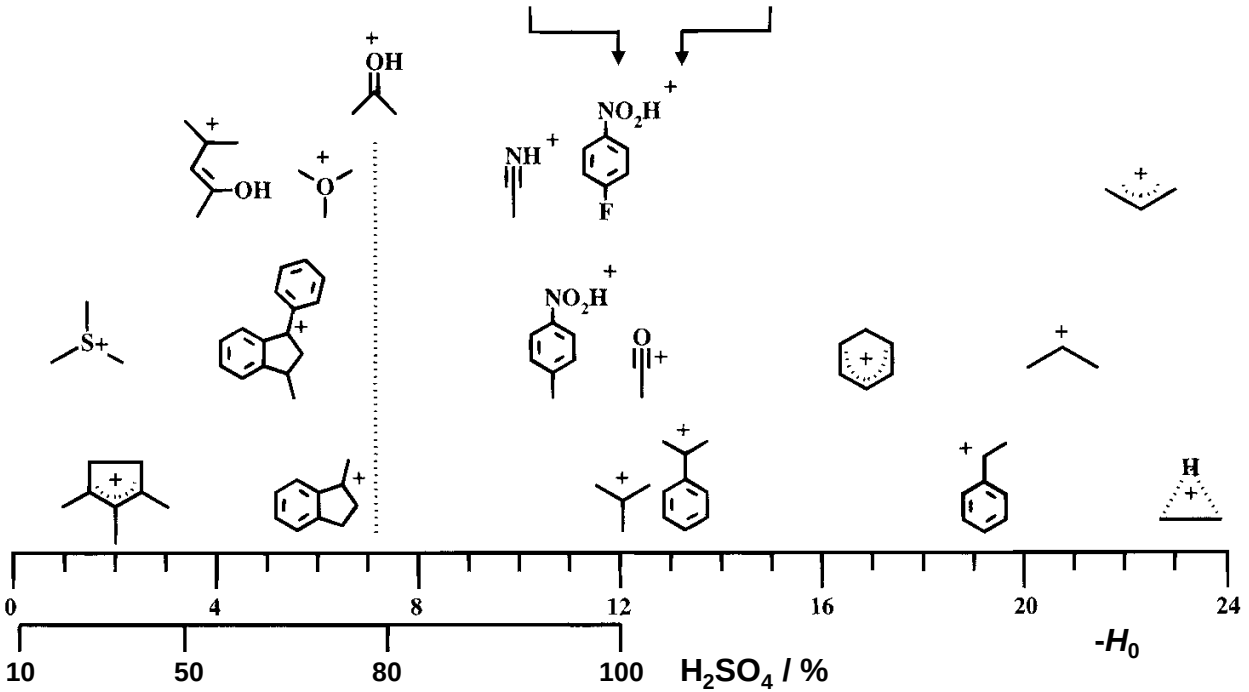

J.F. Haw et al., Acc. Chem. Res. 29 (1996) 259.

III. Tailoring of surface sites

H/D exchange kinetics as an acidity scale

in situ **^{1}H MAS NMR studies of H/D exchange in zeolite H,Na-Y loaded with ethylbenzene ($C_6D_5C_2H_5$)**

stack plot of ^{1}H MAS NMR spectra recorded at *T* = 358 K

B_0 = 9.4 T, ν_0 = 400.1 MHz

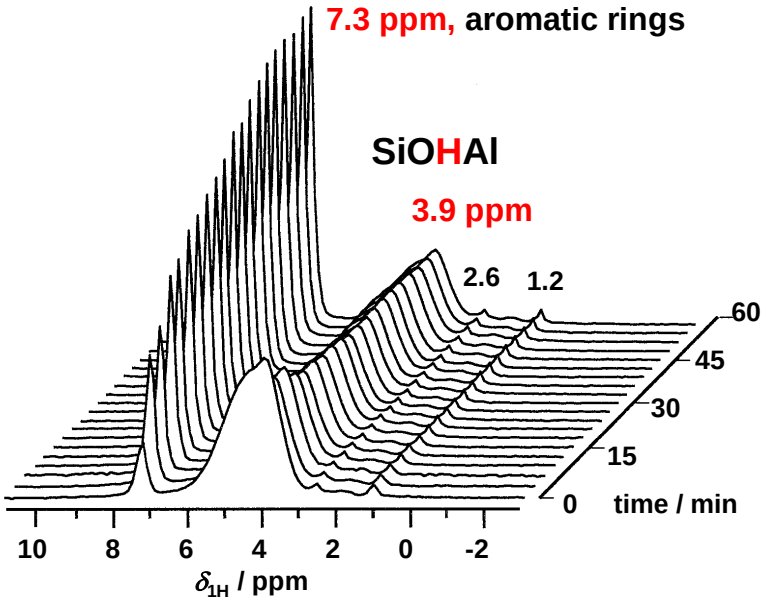

H/D exchange rates at *T* = 328 - 358 K

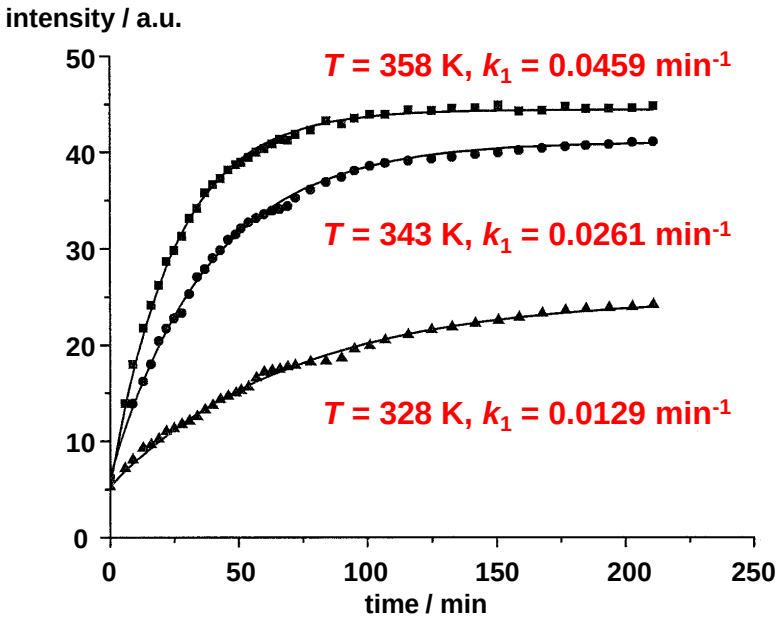

J. Huang et al., Microporous Mesoporous Mater. 99 (2007) 86.

III. Tailoring of surface sites

H/D exchange kinetics as an acidity scale

in situ **^{1}H MAS NMR spectroscopy of H/D exchange in zeolites H,Na-Y (n_{Si}/n_{Al} = 2.7), 75La,Na-Y (n_{Si}/n_{Al} = 2.7), and H-ZSM-5 (n_{Si}/n_{Al} = 26)**

deuterated aromatics on zeolite H,Na-Y

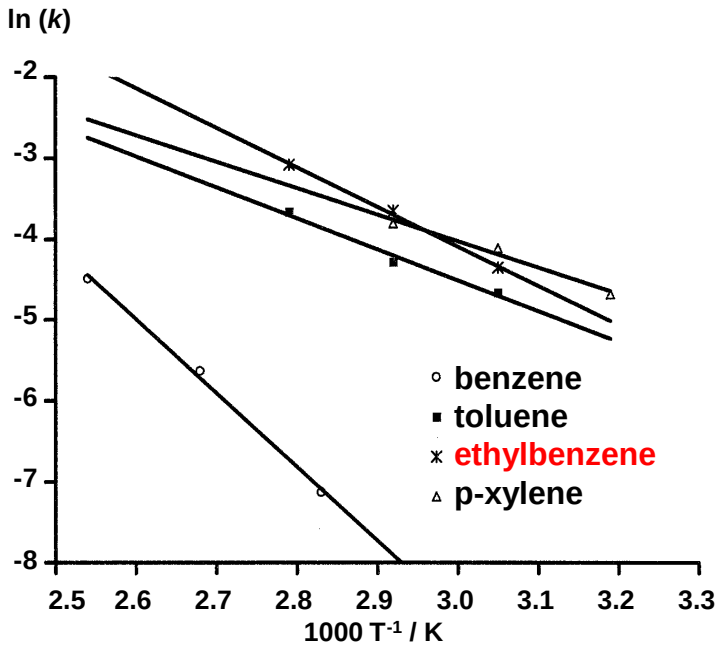

activation energies E_A of H/D exchange and low-field shifts $\Delta\delta_{1H}$ upon adsorption of CD_3CN:

catalyst	molecule	E_A / kJ mol^{-1}	$\Delta\delta_{1H}$ / ppm
H,Na-Y	benzene	76	
	ethylbenzene	41	
	toluene	32	
	p-xylene	27	
H,Na-Y	benzene	76	5.1
La,Na-Y	benzene	67	5.7
H-ZSM-5	benzene	46	7.9

J. Huang et al., Microporous Mesoporous Mater. 99 (2007) 86.

III. Tailoring of surface sites

H/D exchange kinetics as an acidity scale

in situ **^{1}H MAS NMR spectroscopy of H/D exchange in zeolites H,Na-Y (n_{Si}/n_{Al} = 2.7), 75La,Na-Y (n_{Si}/n_{Al} = 2.7), and H-ZSM-5 (n_{Si}/n_{Al} = 26)**

deuterated aromatics on zeolite H,Na-Y

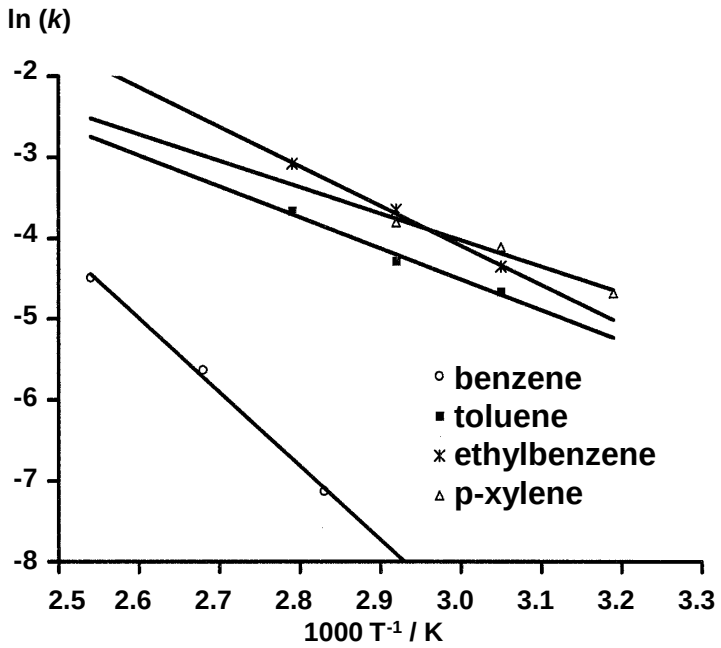

activation energies E_A of H/D exchange and low-field shifts $\Delta\delta_{1H}$ upon adsorption of CD_3CN:

catalyst	molecule	E_A / kJ mol^{-1}	$\Delta\delta_{1H}$ / ppm
H,Na-Y	benzene	76	
	ethylbenzene	41	
	toluene	32	
	p-xylene	27	
H,Na-Y	benzene	76	5.1
La,Na-Y	benzene	67	5.7
H-ZSM-5	benzene	46	7.9

J. Huang et al., Microporous Mesoporous Mater. 99 (2007) 86.

IV. Catalytic investigations

IV. Catalytic investigations

preparation of catalyst samples for *in situ* MAS NMR studies under batch conditions

dehydration, loading, and sealing of the catalyst filled in an MAS NMR rotor inside a vacuum equipment

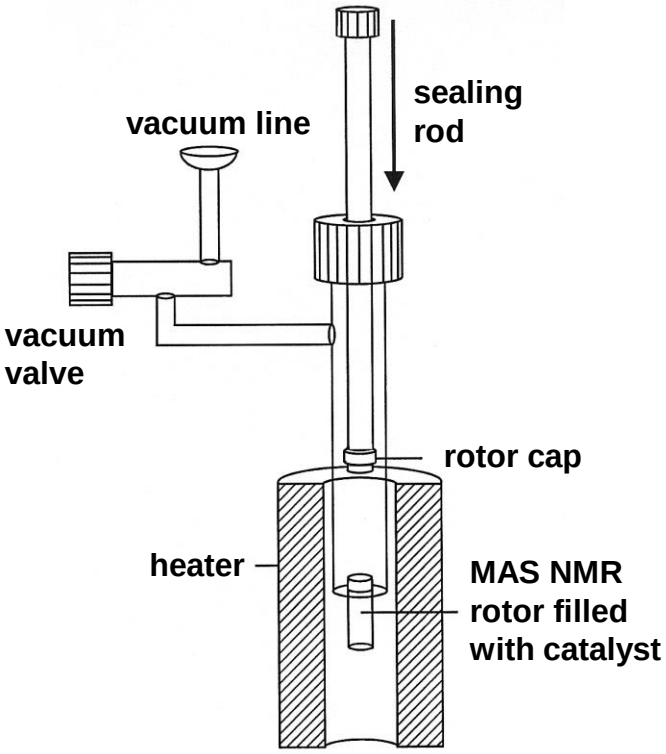

dehydration and loading of the catalyst inside the glass insert (e.g. commercial Wilmad MAS NMR inserts for 4 mm and 7 mm rotors)

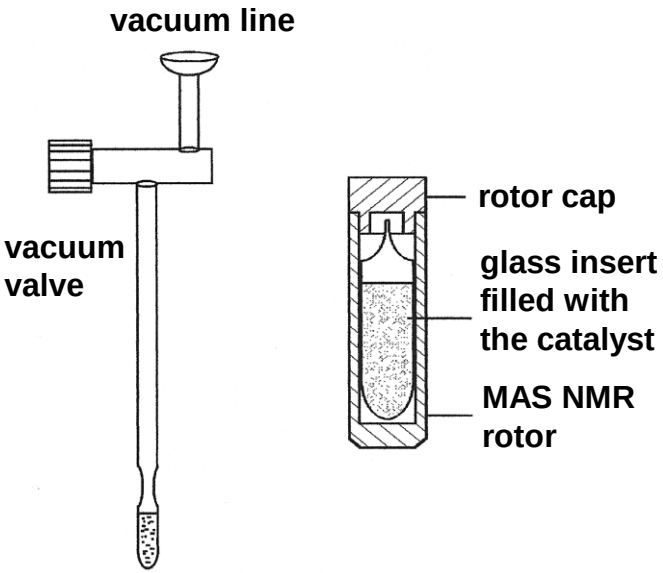

M. Hunger et al., in: B.M. Weckhuysen (ed.), *In situ Spectroscopy of Catalysts*, American Scientific Publishers, Stevenson Ranch, California, 2004, p. 177-218.

IV. Catalytic investigations

mechanisms of the ethylbenzene disproportionation

Streitwieser-Reif mechanism for the homogeneously catalyzed ethylbenzene disproportionation

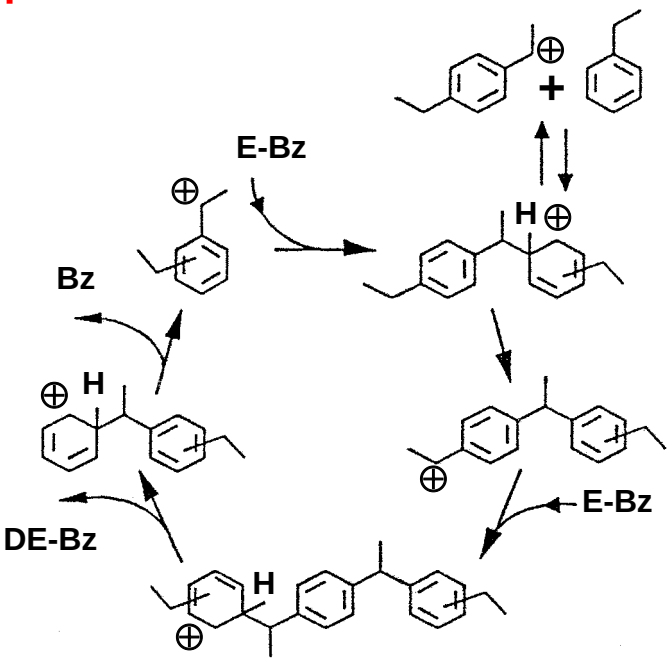

suggested reaction mechanisms for the heterogeneously catalyzed reaction on zeolites:

- ***via*** **diphenylethane intermediates in large-pore zeolites**

- **dealkylation/realkylation with free ethene or alkoxy species in medium-pore zeolites**

U. Weiß et al., Stud. Surf. Sci. Catal., Vol. 105, Elsevier, Amsterdam, 1997, p. 973.

IV. Catalytic investigations

mechanisms of the ethylbenzene disproportionation

^{13}C MAS NMR investigation of the ethylbenzene conversion on large-pore zeolites H,Na-Y and 63Al,Na-Y

^{13}C MAS NMR

H,Na-Y + ethyl[α-^{13}C]benzene

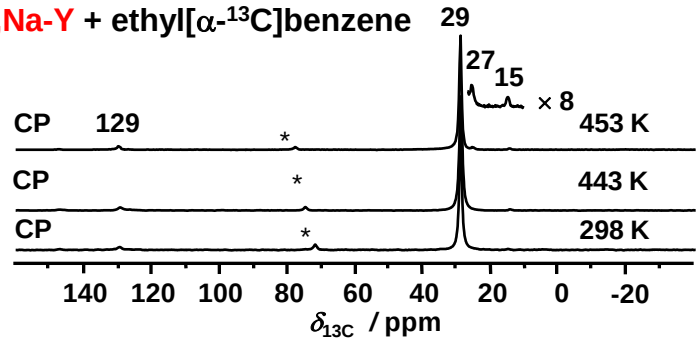

63Al,Na-Y + ethyl[α-^{13}C]benzene

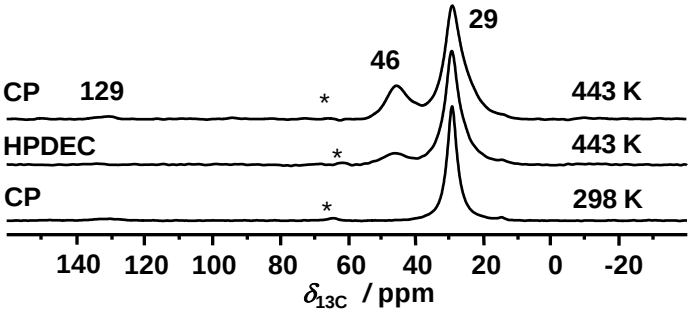

reaction mechanism

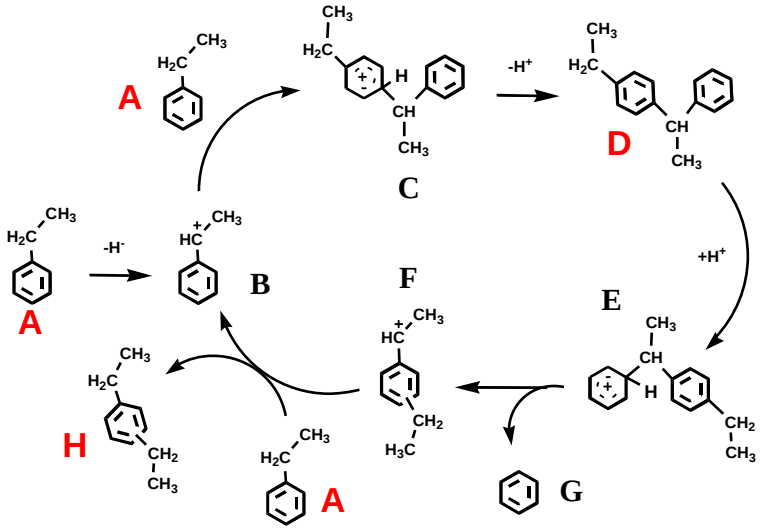

in supercages with diameter of 1.2 nm

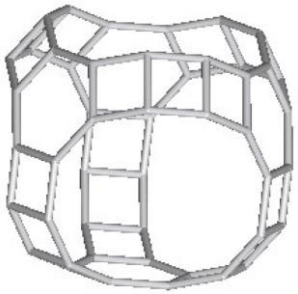

assignment: 27 ppm diethylbenzene (H) 46 ppm diphenylethane (D)
29 ppm ethylbenzene (A) 129 ppm aromatic carbons

J. Huang et al., J. Am. Chem. Soc. 130 (2008) 12642.

IV. Catalytic investigations

mechanisms of the ethylbenzene disproportionation

structure of medium-pore zeolite ZSM-5:

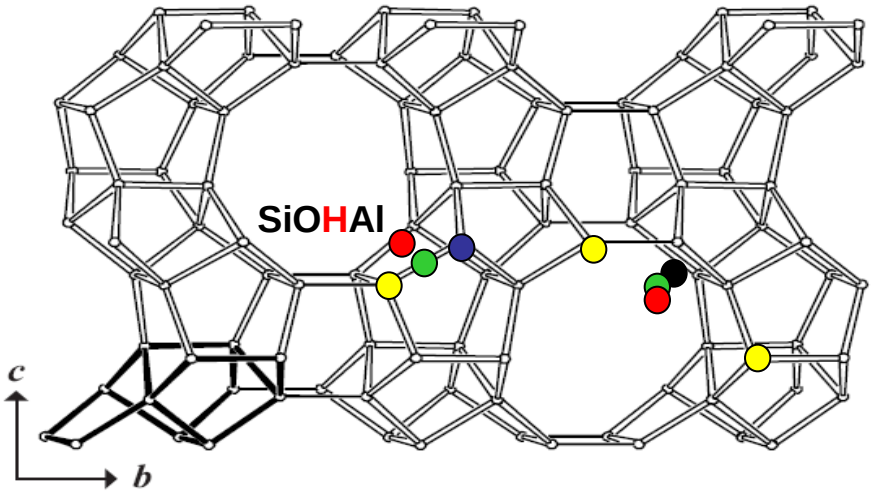

$H^+_n[Al_nSi_{96-n}O_{192}]$

crossing intersections with interconnecting 10-ring channels

[100] 0.51 nm x 0.55 nm

[010] 0.53 nm x 0.56 nm

Al atom
Si atom
O atom
H atom
extra-framework cations (Na^+, Al^{3+} etc.)

IV. Catalytic investigations

mechanism of the ethylbenzene disproportionation

^{13}C MAS NMR investigation of the ethylbenzene conversion on medium-pore zeolite ZSM-5

^{13}C MAS NMR mechanism

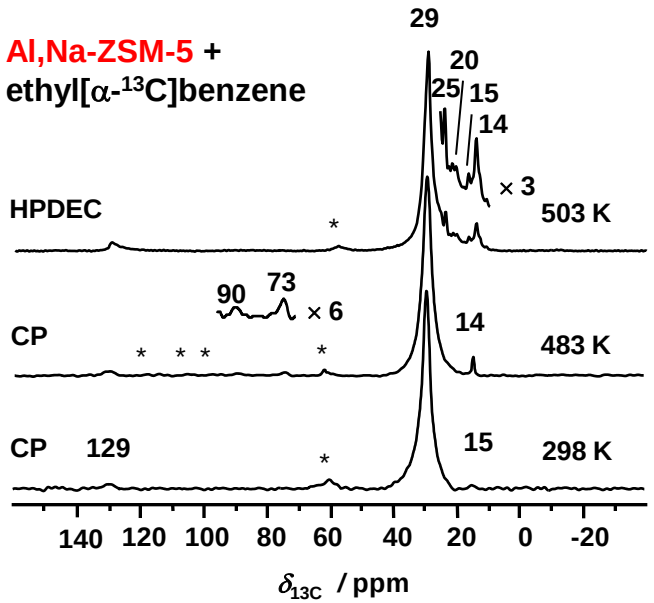

reaction

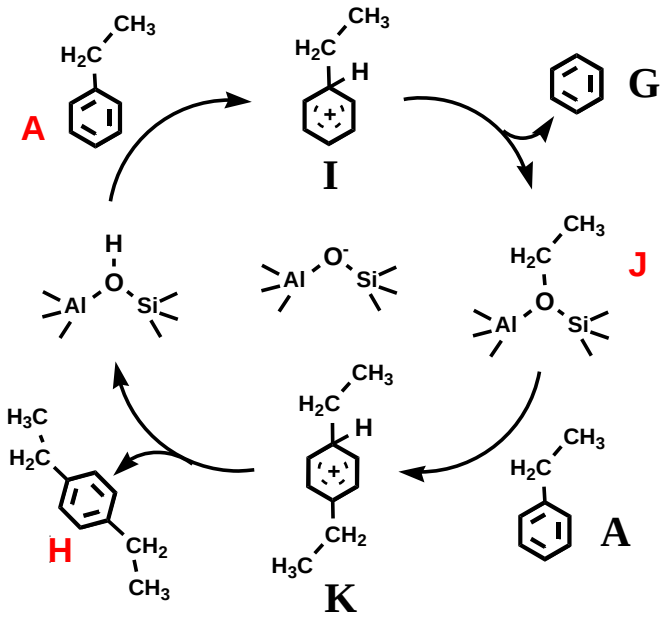

assignment:

25 ppm	diethylbenzene (H)	73 ppm	surface ^{13}C-1-ethoxy groups (J)
29 ppm	ethylbenzene (A)	90 ppm	oligomeric alkoxy groups
		129 ppm	aromatic carbons

J. Huang et al., J. Am. Chem. Soc. 130 (2008) 12642.

IV. Catalytic investigations

continuous-flow (CF) and pulsed-flow (PF) MAS NMR spectroscopy

coupling of MAS NMR and UV/Vis spectroscopy by installation of a quartz fiber at the bottom of the MAS NMR stator

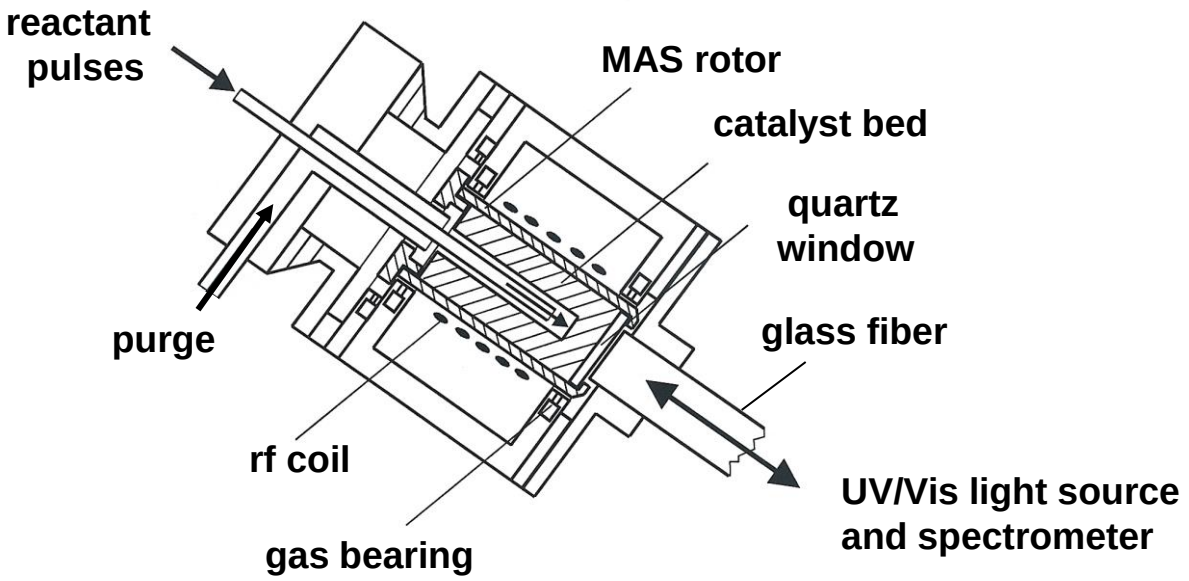

M. Hunger, Prog. Nucl. Magn. Reson. Spectrosc. 53 (2008) 105.

IV. Catalytic investigations

continuous-flow (CF) and pulsed-flow (PF) MAS NMR spectroscopy

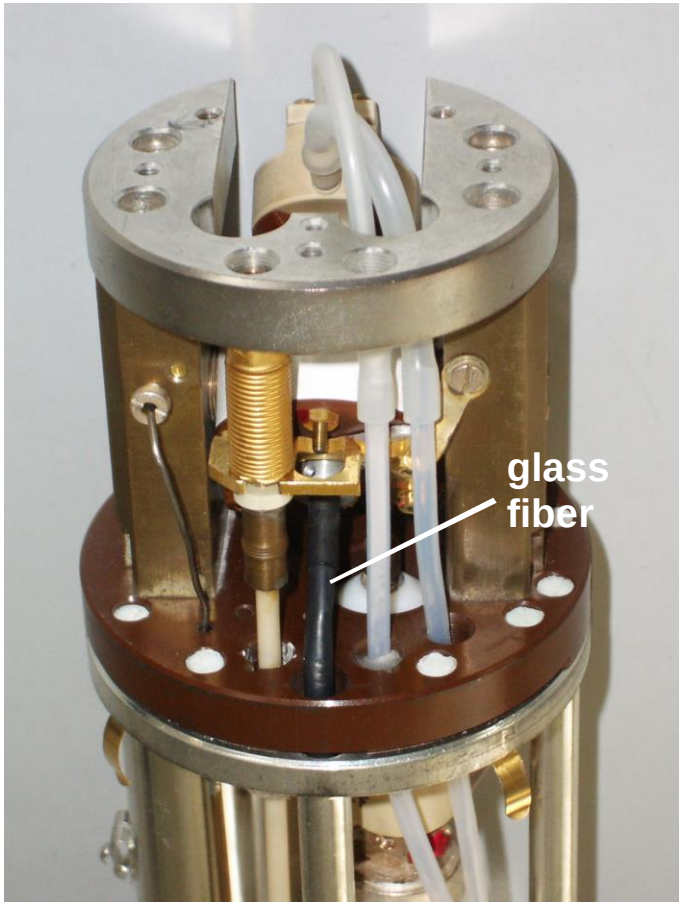

7 mm Bruker MAS NMR probe equipped with a glass fiber (left) and UV/Vis light source and spectrometer of Avantes (bottom)

M. Hunger, Prog. Nucl. Magn. Reson. Spectrosc. 53 (2008) 105.

IV. Catalytic investigations

continuous-flow (CF) MAS NMR spectroscopy

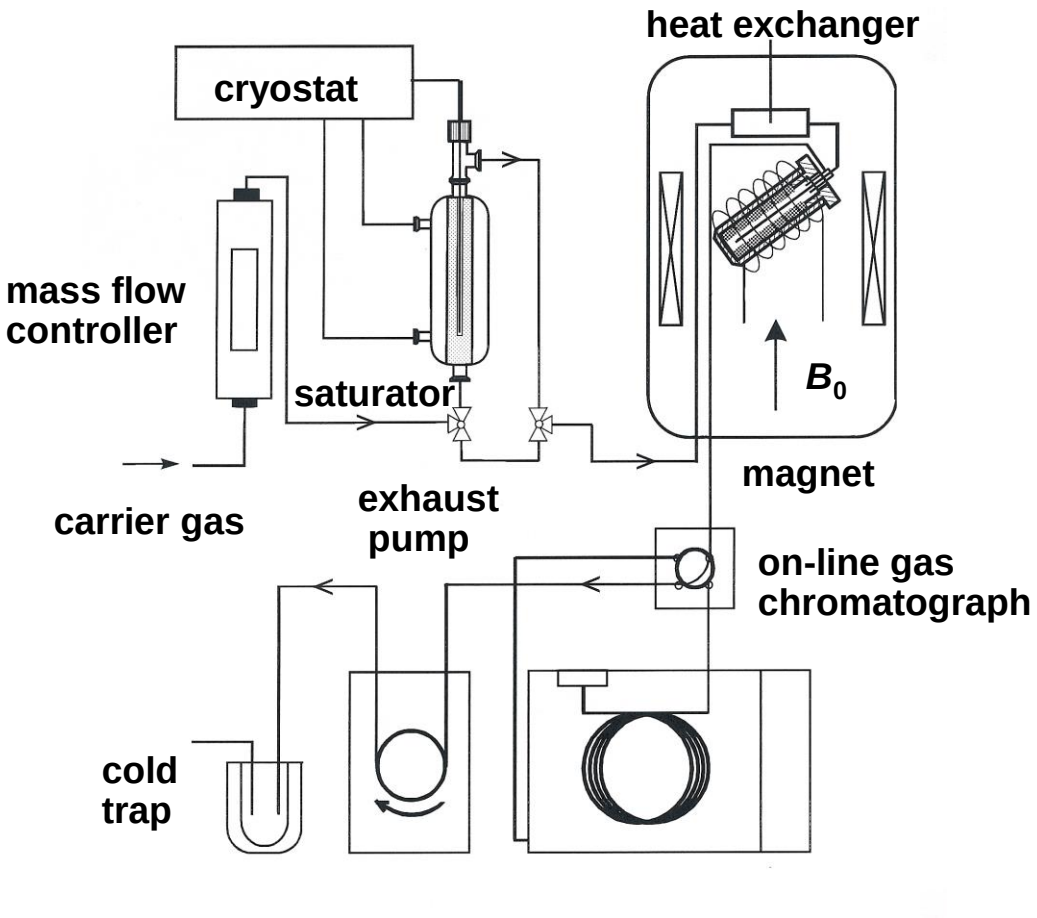

M. Hunger, Prog. Nucl. Magn. Reson. Spectrosc. 53 (2008) 105.

IV. Catalytic investigations

pulsed-flow (PF) MAS NMR spectroscopy

connection of a micro pump with the *in situ* MAS NMR probe

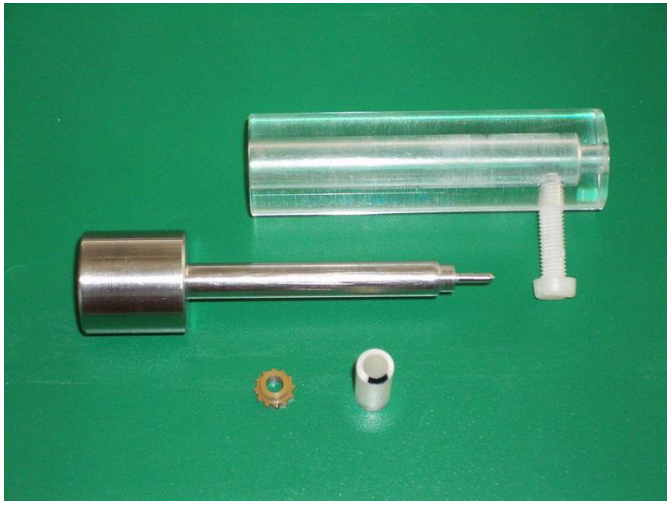

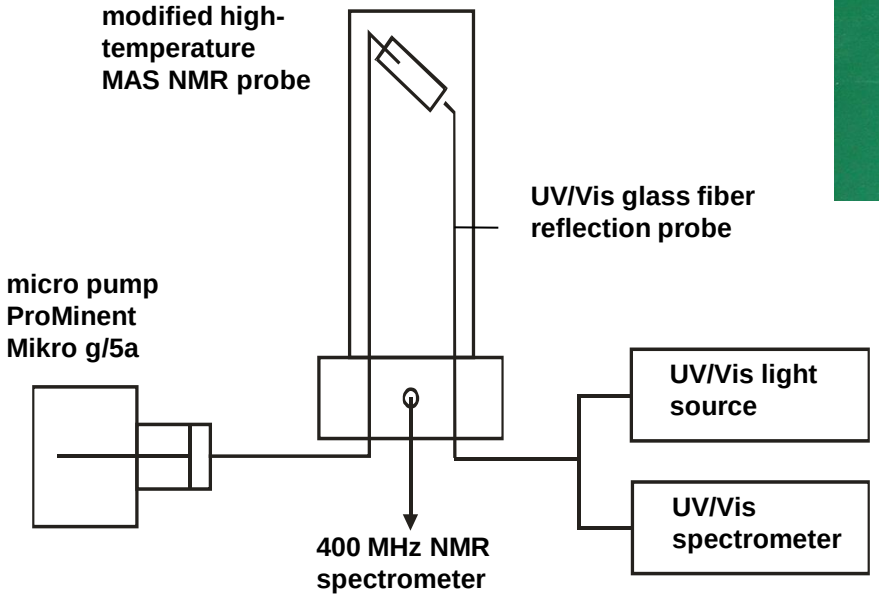

M. Hunger, Prog. Nucl. Magn. Reson. Spectrosc. 53 (2008) 105.

IV. Catalytic investigations

pulsed-flow (PF) MAS NMR-UV/Vis spectroscopy

injection of liquid reactants into the spinning MAS NMR rotor *via* a micro-pulse pump

pulsed-flow experiment

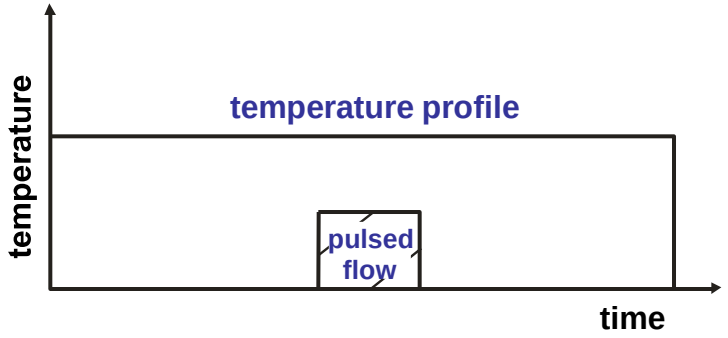

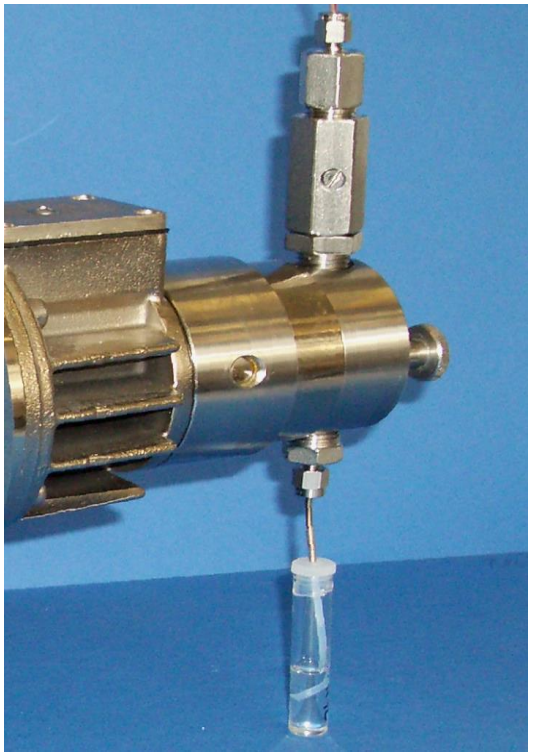

pulsed-flow experiments:

- study of the time dependence of the conversion of reactants

- study of the isotopic exchange of reactants at high temperatures with well-defined starting time

pump Mikro g/5 of Fa. ProMinent, Germany, for single pulses with volumes of 2 to 50 µl

IV. Catalytic investigations

mechanism of the methanol-to-olefin (MTO) conversion on acidic zeolites

via **olefinic compounds (H. Schulz, M. Wei, Microporous Mesoporous Mater. 29 (1999) 205)**

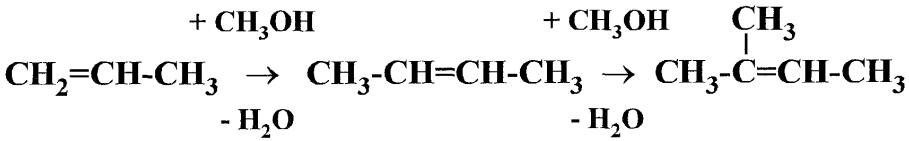

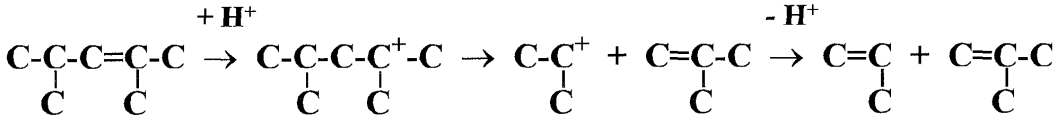

via **polyalkylaromatics (J.F. Haw et al., Acc. Chem. Res. 36 (2003) 317)**

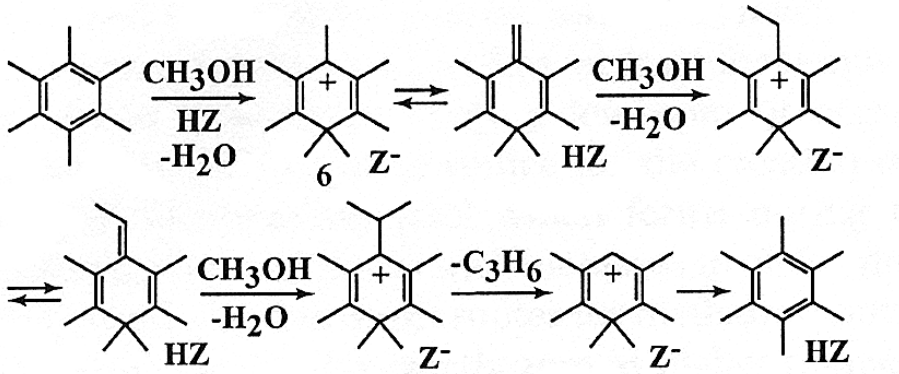

IV. Catalytic investigations

mechanism of the methanol-to-olefin (MTO) conversion on acidic zeolites

H-ZSM-5: Structure type MFI

$H^+_n[Al_nSi_{96-n}O_{192}]$

crossing intersections at

interconnecting 10-ring channels

[100] 0.51 nm x 0.55 nm

[010] 0.53 nm x 0.56 nm

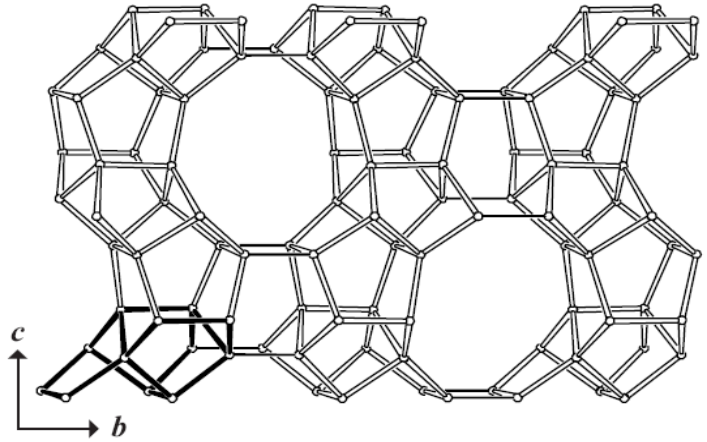

H-SAPO-34: Structure type CHA

$H^+_n[Al_{18}P_{18-n}Si_nO_{72}]$

chabazite cages accessible by

8-ring windows perpendicular to

[001] 0.38 nm x 0.38 nm

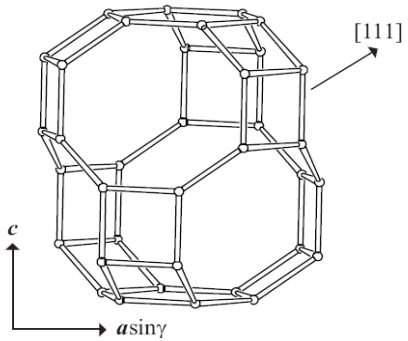

chabazite cage

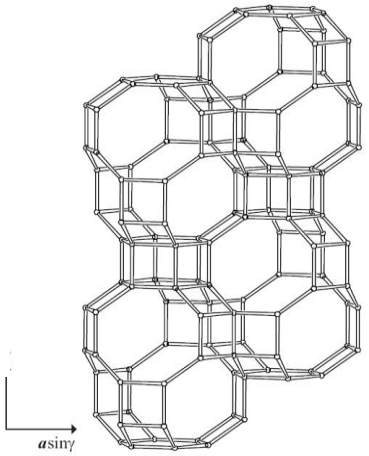

IV. Catalytic investigations

mechanism of the methanol-to-olefin (MTO) conversion on acidic zeolites

***in situ* CF ^{13}C MAS NMR study of ZSM-5 (W_{cat}/F_{me} = 25 gh/mol)**

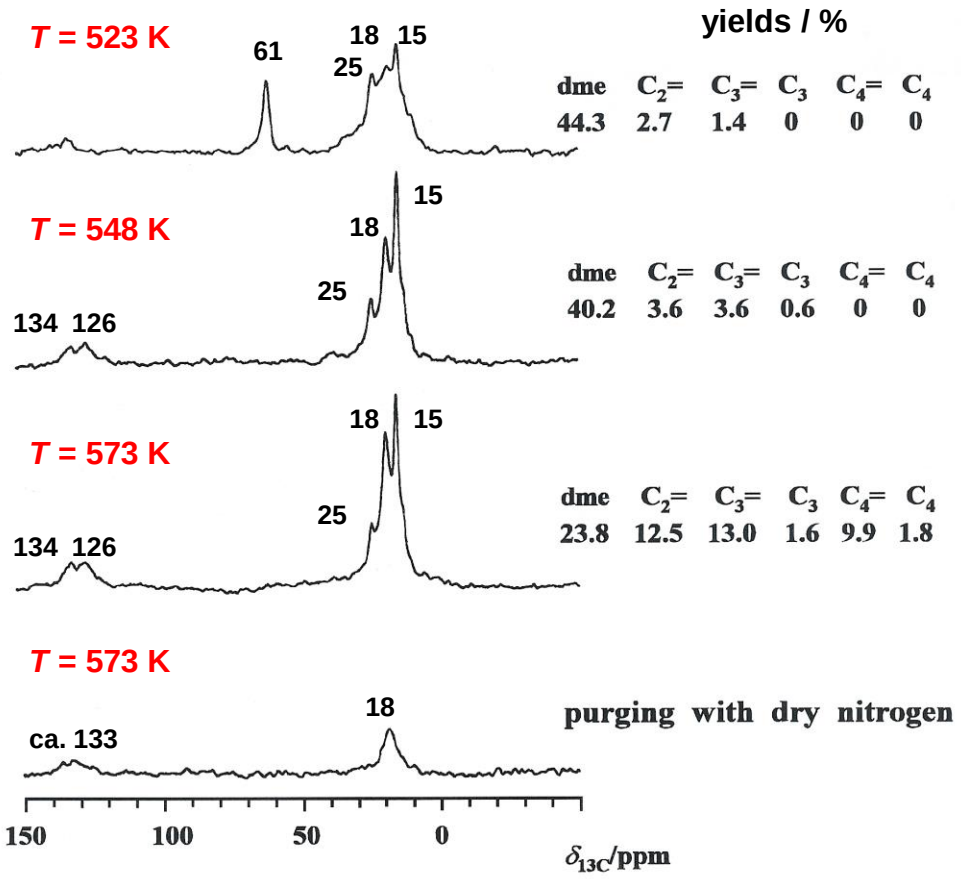

$T \lesssim$ 548 K:

mixture of olefinic and aromatic compounds, such as:
- 3-hexene (14.4, 25.9, 131.2 ppm)
- 2,4-hexadiene (17.2, 126.2, 132.5 ppm)
- ….
- hexamethylbenzene (17.6, 132.1 ppm)

T = 573 K:

polymethylaromatics remain after purging, such as:
- toluene (20.3, 128.5, 129.0 ppm)
- ....
- hexamethylbenzene (17.6, 132.1 ppm)

IV. Catalytic investigations

mechanism of the methanol-to-olefin (MTO) conversion on acidic zeolites

***in situ* CF ^{13}C MAS NMR study of SAPO34 (W_{cat}/F_{me} = 25 gh/mol)**

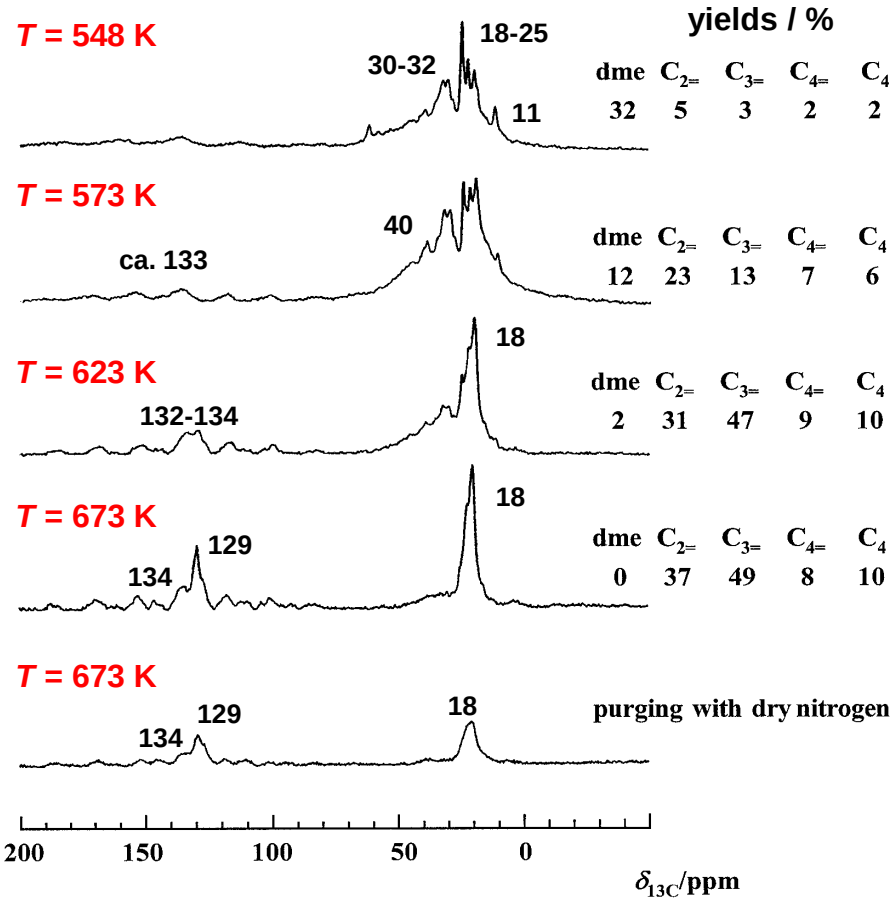

***T* ≤ 573 K:**

mixture of olefinic and aromatic compounds, such as:

- **2-methyl-2-butene (9.3-22.5, 118.8, 131.8 ppm)**
- **2,4-hexadiene (19.5, 132.5 ppm)**
- **….**
- **tetramethylbenzene (18.9, 131.1, 134.0 ppm)**

***T* > 573 K:**

domination of polymethyl-aromatics, such as:

- **toluene (20.3, 128.5, 129.0 ppm)**
- **....**
- **trimethylbenzene (21.2, 127.4, 137.6 ppm)**
- **hexamethylbenzene (17.6, 132.1 ppm)**

IV. Catalytic investigations

mechanism of the methanol-to-olefin (MTO) conversion on acidic zeolites

comparing study of organic deposits formed on H-SAPO-34 (W_{cat}/F_{me} = 25 gh/mol)

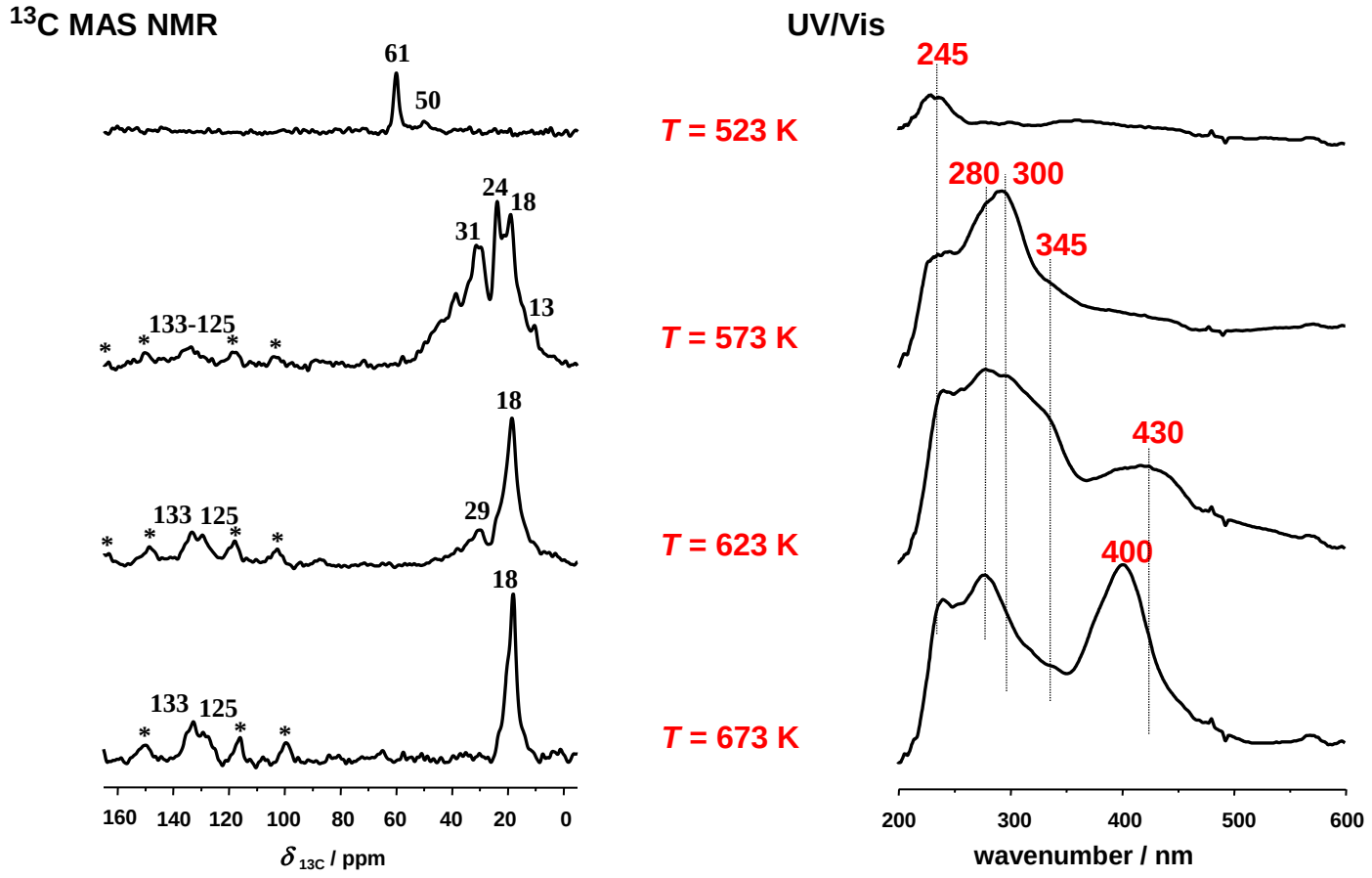

245 nm: dienes
280 nm: polyalkylaromatics
300 nm: monoenylic carbenium
345 nm: dienylic carbenium
400 nm: polycyclic coke
430 nm: trienylic carbenium

Y. Jiang et al., Microporous Mesoporous Mater. 105 (2007) 132.

IV. Catalytic investigations

side-chain H/D exchange of ethylbenzene on steamed zeolite deH,Na-Y/81.5

$C_6H_5CD_2CD_3$ + *n* SiOHAl ⟶ $C_6H_5CDHCD_2H$ + *n* SiODAl

7.3 ppm 3.8 ppm 2.7 ppm 1.2 ppm

***in situ* PF ^{1}H MAS NMR experiments:**

- pulses of 7.8 mg ethyl-d_5-benzene
- 32 scans per spectrum with repetition time of 10 s at 9.4 T
- sample spinning rate of *ca.* 2 kHz

message:

- regioselective H/D exchange at 443 to 463 K (^{1}H MAS NMR)
- different types of carbenium ions (UV/Vis)

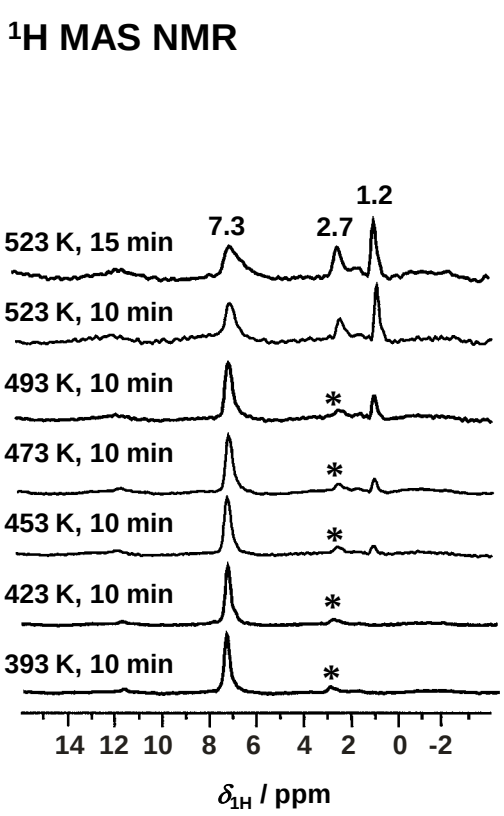

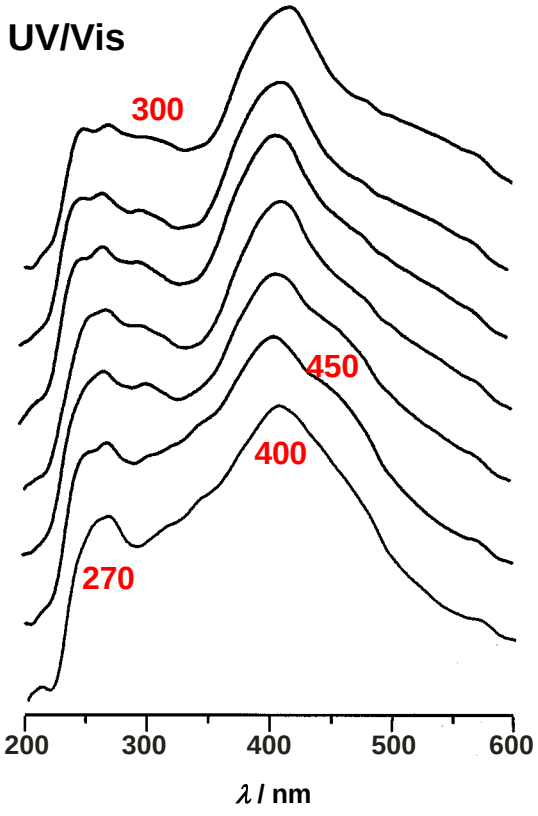

J. Huang et al., ChemPhysChem 9 (2008) 1107.

IV. Catalytic investigations

side-chain H/D exchange of ethylbenzene on steamed zeolite deH,Na-Y/81.5

$C_6H_5CD_2CD_3$ on dealuminated zeolite deH,Na-Y/81.5 (24.5 Al^{ex}/u.c, 10.9 SiOHAl /u.c)

***in situ* PF ^{1}H MAS NMR**

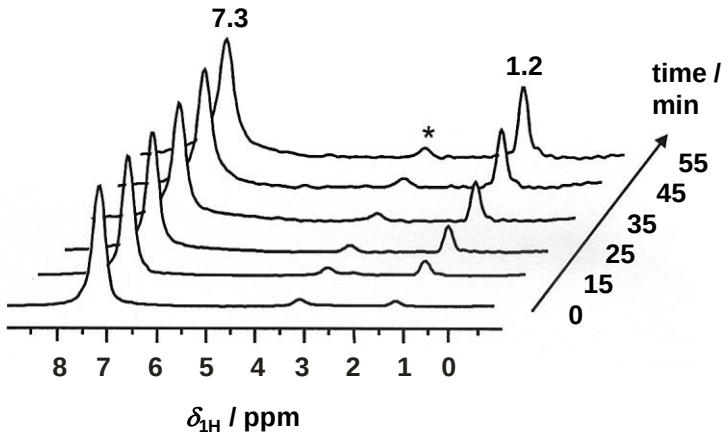

Arrhenius plot

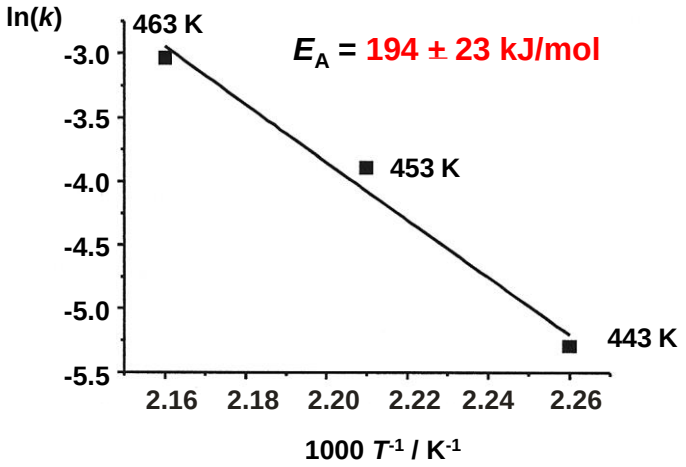

activation energy of the regioselective H/D exchange (194 kJ/mol) indicates that a hydride transfer reaction is the rate determining step

J. Huang et al., ChemPhysChem 9 (2008) 1107.

IV. Catalytic investigations

side-chain H/D exchange of ethylbenzene on steamed zeolite deH,Na-Y/81.5

^{1}H MAS NMR:

- **selective H/D exchange of methyl groups (1.2 ppm)**
- **activation energy of 194 kJ/mol indicates hydride transfer**

UV/Vis:

- **ethylcyclohexadienyl carbenium ions at BAS (400 nm), A**
- **sec-ethylphenyl carbenium ions at LAS (450 nm), B**
- **styrene at BAS (300 nm), C**

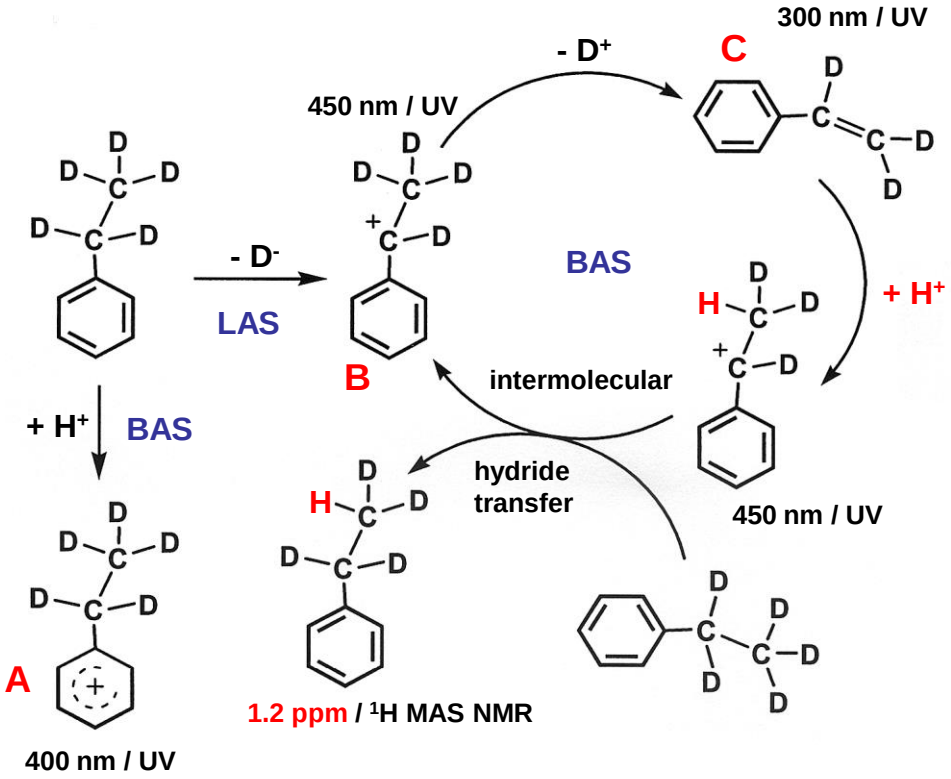

BAS: Broensted acid site **LAS: Lewis acid site**

J. Huang et al., ChemPhysChem 9 (2008) 1107.

Solid-state NMR of solid catalysts

I. Synthesis of catalysts ⟷
- nature and local structure of framework atoms
- framework defects, amorphous phases and impurities

↓

II. Framework modification ⟷
- incorporation and release of framework atoms
- nature and location of extra-framework species and cations
- anchoring of organic compounds

↓

III. Tailoring of surface sites ⟷
- number, strength, and accessibility of Brønsted acid sites
- presence and strength of base sites
- presence of Lewis acid sites

↓

IV. Catalytic investigations ⟷
- adsorbate complexes and intermediates formed on catalysts
- reaction mechanisms
- reasons of catalyst deactivation

↓

topics I to III

Thanks to ….

co-workers:

Thomas Horvath
Michael Seiler
Andreas Buchholz
Udo Schenk
Mingcan Xu
Jiang Jiao
Jun Huang
Yijiao Jiang
Jörg Frey
Arne Bressel
Reddy Marthala
Bejoy Thomas
Wei Wang
Yean Sang Ooi
Harald Henning
Weili Dai
Zichun Wang
u.a.

financial support:

Deutsche Forschungs-gemeinschaft

Fonds der Chemischen Industrie

Volkswagen Foundation

DECHEMA e.V.

Alexander von Humboldt-Foundation

u.a.

Thanks to ….